# Investigating the potential use of satellite remote sensing for phenological differentiation of Arctic vegetation on the Kola Peninsula, Russia

Charlotte Daffern

MPhil Polar Studies

Scott Polar Research Institute

University of Cambridge

June 2017

Front page image credit: Vasiliy Saprykin (http://briard.ru/en/map/muo.php)

# Acknowledgements

Many thanks to Gareth Rees for his support in developing this project, and for the time spent imparting technical wisdom on the use of Matlab and QGIS. Thanks also to Gabriel Amable for providing advice on the acquisition and preparation of MODIS imagery using the MODIS Reprojection Tool, and to Tejas Guruswamy for helping ensure that my image analysis code was fit for purpose.

The MODIS scenes used in this research were retrieved from the online EarthExplorer website, courtesy of the NASA EOSDIS Land Processes Distributed Active Archive Center (LP DAAC), USGS/Earth Resources Observation and Science (EROS) Center, Sioux Falls, South Dakota, https://lpdaac.usgs.gov/.

# Table of Contents

# List of Figures

# List of Tables



# List of Equations

# 1 – Introduction

The tundra-taiga ecotone (also known as the tundra-taiga interface or boundary; henceforth referred to as 'the TTE' or 'the ecotone') is a transitional vegetation zone which is present on a circum-Arctic scale, spanning over 13,400 km of the terrestrial biosphere between latitudes of approximately 60 to 70˚N across North America and Eurasia (Callaghan *et al*, 2002; Virtanen *et al*, 2016). The ecotone describes the non-linear boundary between the boreal forests of the taiga biome and the low, shrubby vegetation of the tundra biome. Broadly speaking the transition occurs along a south-north axis from taiga to tundra, typified by decreasing tree density, height and growth rates, though this is spatially variable due to the influence of factors including climate, continentality and relief (Sveinbjornsson *et al*, 2002). The two biomes forming the TTE have significantly different vegetative properties which fulfil different roles within the global biosphere, and therefore contribute to different feedback effects with significant responses to and implications for climate change (Harding *et al*, 2002). The broad narrative surrounding the TTE predicts northwards expansion of the boreal forests at the expense of tundra squeeze to the north. Attempts to suitably quantify any such migration of the biome boundary are ongoing, with efforts in the research area increasingly aware of the need to improve understanding of methodological limitations, in order to better constrain uncertainties surrounding the complex physical changes that have been occurring at the ecotone in recent years (Montesano *et al*, 2016).

This study will use a novel approach to analysing NDVI data acquired using satellite remote sensing, based on parameterization of annual phenology, with two major purposes:

1. To investigate the effectiveness of the newly developed methodology, particularly with regard to exploring the potential of phenological parameters as a means of differentiating between tundra and taiga vegetation.
2. To apply the developed methodology to a region of the Arctic TTE in order to undertake an empirical assessment of its potential for predicting vegetation cover based on the normalized difference vegetation index (NDVI).

The Kola Peninsula has been selected as the site for this work for a number of reasons: firstly, the availability of pre-existing research in the area supports a working knowledge of the vegetation distributions, and key environmental drivers such as climate and relief; secondly, vegetation gradients driven by altitude and anthropogenic factors exist at well-mapped locations within the region, providing interesting and informative cases for application of the new methodology; and thirdly, the results of this project will support ongoing research into vegetation change on the peninsula, with a view to expanding the scope of the research in the future to diverse areas of the circumpolar TTE.

## 1.1 Rationale

Studying the TTE contributes to two major strands of Arctic environmental research, which form the basis for this project. Firstly, changes in TTE location in response to climate change can be used as an indicator of high latitude climate change, as climate is a primary control on vegetation growth. Secondly, migration of the TTE can be used as an indicator of changes to the area of the two biomes, potentially describing variation in the relative importance of each. This is important due to the different properties of the two biomes, including albedo, carbon storage, and constituent plant functional types. Herein a broad overview of the roles of Arctic vegetation within an integrated global system of biophysical feedbacks will be followed by a discussion of pre-existing methodologies for investigating the TTE, and the results of such studies. This will frame the present research, allowing for a discussion around why the use of phenology based on NDVI extracted from data acquired by the Moderate Resolution Imaging Spectroradiometer (MODIS) remote sensing instrument has the potential to be usefully applied to this subject matter.

### What is the importance of studying the tundra-taiga ecotone?

At present, Arctic biomes are net sinks of carbon, with large stocks held in the soil as well as in the standing biomass of vegetation. Estimates suggest that one third of fossil fuel emissions globally are taken up by tree growth, with boreal forests responsible for up to 50% of this total (Pan *et al*, 2011; Malhi *et al*, 1999). One study by Post *et al* (1982) estimated the soil carbon pools of the taiga and tundra biomes at approximately 181 Pg and 191.8 Pg respectively. A more recent study estimates that the northern circumpolar permafrost region as a whole contains 1672 Pg of organic carbon (Tarnocai *et al*, 2009). Bradshaw and Warkentin (2015) give values ranging from 367.3 to 1715.8 Pg for the boreal forests alone. These more recent results are both significantly higher than the combined results of earlier studies, suggesting that as methodologies for quantifying carbon storage advance, an improved understanding of the importance of high latitude stores is achieved (Jobbagy and Jackson, 2000; Apps *et al*, 1993).

The long-term future of these major stores of carbon are the subject of speculation, and are often considered to be in doubt due to ongoing climatic changes. This raises issues of potentially large atmospheric carbon additions, which could further contribute to atmospheric warming due to the nature of the released carbon as carbon dioxide ($CO_2$) and methane ($CH_4$), both major greenhouse gases (Billings, 1987; Tarnocai *et al*, 2009). Carbon cycling in high latitude forests is currently temperature-limited; with climatic warming reported and expected to continue at an accelerated rate in these areas, there is speculation that the decomposition

rates of organic matter in these environments will increase, reducing the capacity of this carbon store (Deluca and Boisvenue, 2012).

It has been estimated that transitions in the biophysical functioning of the boreal forests will cause them to transition from sinks to sources of carbon on the scale of 70 to 100 years (Hopkinson *et al*, 2016). However, multiple studies argue that this transition will be undergone sooner, or indeed that it may have already occurred. A 90-year study at a site in Finland has shown that recent biomass sequestration associated with an increase in boreal forest growing stock has been insufficient to offset fossil $CO_2$ emissions (Kauppi *et al*, 2010). Wang and Polglase (1995) found that over a study period of 140 years both tundra and taiga vegetation zones switched between carbon sinks and carbon sources multiple times. This occurred most recently in the 1980s, when both biomes entered carbon source states. Independent evidence has been found showing that a decrease in boreal forest carbon uptake has occurred since the 1980s, which supports this work (Bradshaw and Warkentin, 2015). A feedback loop has also been identified suggesting that the release of soil nutrients due to climate warming could amplify significant carbon release from deep soil layers, suggesting a positive feedback loop of net carbon loss from high latitude soil that will be triggered by high latitude warming (Mack *et al*, 2004). Melting of permafrost layers also has significant implications for the hydrology of Arctic areas. Paludification is expected to become an increasingly prominent factor in the future of the TTE due to increased episodes of prolonged winter flooding, associated with pressuring of the climatic limits of the boreal forests (Crawford *et al*, 2003). Soil moisture content and drainage is also associated with the ability of boreal forest areas to accumulate and store carbon, linked to the colonization of different moss species (Harden *et al*, 1997).

Albedo is another prominent reason that studying the TTE is important, due to the major role it fulfils in the climate system in controlling how solar radiation interacts with the surface of the earth. The optical characteristics of Arctic vegetation types vary significantly, and the snow cover regime associated with each biome can further exacerbate differences in albedo on inter-annual time scales. This results in a coupling of vegetation and climate on regional scales with significant long-term implications (Bonan *et al*, 1995).

Low, shrubby tundra vegetation generally has a higher albedo than taiga forests. In taiga forests, the pigmentation of the composite plant species is darker and the percentage vegetation cover in terms of leaf area index is higher than in tundra areas, both of which cause relatively decreased albedo (Bonan *et al*, 1995). The tundra biome is also characterized by shorter snow-free periods during the summer months in comparison to the taiga biome, partly due to the insulating effect of taiga forests on the ground surface resulting in elevated temperatures which promote earlier snow melt, and partly due to the lower profile tundra

vegetation becoming more easily submerged beneath a snow layer (Sturm *et al*, 2005; Bonan *et al*, 1992). These factors result in significantly higher absorption of incoming shortwave solar radiation over longer periods of time over each annual seasonal cycle for taiga vegetation compared to tundra. In combination with plant structural changes affecting latent heat flux from evapotranspiration, taiga vegetation produces a much more significant net positive forcing effect on the temperature of the atmosphere than tundra vegetation (Beringer *et al*, 2005). Whilst vegetation changes only directly influence climate on local to regional scales, the extent of the surface area of the northern hemisphere covered by the tundra and taiga biomes causes the cumulative effect of these variations to have a considerable impact on the global climate system (Loranty *et al*, 2011; Lundberg and Beringer, 2005; Sturm *et al*, 2005).

In summary, knowledge of the position and movement of the TTE is useful as it represents transformation between tundra and taiga environments. This has implications for both the long-term storage of soil carbon, and the volume of standing biomass stocks. Changes in vegetation type also have significant impacts on albedo, partly due to patterns of annual snow cover variability, which has wide-reaching consequences for the global energy budget. Studying variation in TTE location and form therefore provides crucial information on both climate change responses and the associated forcing feedbacks over a region of the globe which is particularly susceptible to such changes.

## What results have been gathered by previous research into the tundra-taiga ecotone?

The significance of the tundra and taiga biomes in climate change and biogeographical research has been known for a number of years, and therefore a body of literature exists exploring how and why the TTE has changed in recent times. However, there are no standardized methods for application to this problem area. A key area of advancement in recent decades has been the application of remote sensing to high latitude vegetation studies; the continual development of new airborne and satellite sensors is a primary cause of the need for ongoing exploration of new methodologies for researching the TTE. A summary of the major remote sensing platforms used in studying the TTE is available from Daffern (2016). Due to the rapid development of these new remote sensing technologies, much of the research into the TTE remains focussed on assessing methodological limitations, and so reports of the state of the ecotone are somewhat limited, and are rarely presented as definitive. The results of pertinent studies are presented here to provide a review of the breadth of ongoing research, with results detailing ecotone change given where possible.

It is important to note that the lack of cohesive methodologies is a limiting factor in undertaking comparative assessment of existing research due to the fact that the results of

these studies are often presented in different ways, and expressed in a variety of units. This is particularly pronounced due to the diversity of spatial, temporal and spectral resolutions of remote sensing data used to study the TTE, alongside numerous other data sources such as historical forest maps. Further complications are introduced due to the fact that these data sources are applied using different methodologies to study ranges which vary in temporal and spatial extent. Whilst some studies of the TTE focus on change in spatial location through time based on spectral variation, others focus on *in situ* changes to the phenological characteristics of the vegetation. Studies investigating variation in TTE form – rather than just location – as a means of analysing vegetation response to climatic drivers have become increasingly prevalent over the past ten to fifteen years due to an improved appreciation of the complexity of the ecotone as a vegetation gradient, not simply a geographical boundary.

Studies investigating changes in the spatial location of the tundra-taiga transition generally find advance of the taiga biome occurring on regional scales. However large variations exist in the measured rates of change, which are often non-uniform and non-linear even within individual studies. For example, Hofgaard *et al* (2013) analysed birch and pine forest lines in northern Norway between 1914 and 2009, finding average northward advancement rates of 156 and 71 m $yr^{-1}$ for the two species respectively. A separate analysis in the same study found significant variations in treeline advance, with birch treeline advance reaching up to 340 m $yr^{-1}$ at some points, whereas the pine treeline only showed advance of 10 m $yr^{-1}$ at some points – which is equal to the uncertainty in the rates of change associated with data source errors. The spatial extent of this study was approximately 500 km longitudinally, representing only around 3% of the TTE. This must be a consideration when scaling between the results of individual studies of the ecotone on regional scales, and the application of these results to broader scales of investigation; wariness should be exercised when considering extrapolating results from one area of the TTE to the circumpolar scales of interest for global vegetation and climate modelling. This study also simplifies the TTE to a pair of lines, delineating absolute transitions in vegetation characteristics which do not realistically exist in the environment (Ranson *et al*, 2011). It is also important to note that a variety of data sources including remote sensing and historical maps were used to construct this time series of change – studies using only remote sensing will not provide information over such long periods, due to the relative youth of the technology.

Attempts to avoid simplifications are the cause of increased efforts to investigate spatial and temporal variation in TTE form as a means of better characterising how high latitude vegetation responds to climate change (Heiskanen, 2006). This is particularly useful as gradients in vegetation often follow gradients in environmental factors such as climate. Since the 1980s, in an area of the TTE responding to altitudinal forcing, Kharuk *et al* (2007) found that marginal

forests have become denser, with krummholz stands transforming to arboreal forms. Tree regeneration resulted in forest propagation into previously tundra areas at a rate of ~1.0-2.0 m $yr^{-1}$, surpassing historical treeline limits by up to 80 m in elevation. Furthermore, the species composition of the forest shifts between larch- and pine-dominance depending on climatic variables including temperature and precipitation.

The study undertaken by Kharuk *et al* (2007) is fairly isolated in its spatial scope due to the methodological limitations of a non-remote sensing based approach. This is a major driver behind the fact that much of the work investigating variation in TTE form is based on remote sensing approaches, which could facilitate global scale applications. For example, the theoretical basis of analysing TTE form rather than just location underpins the work of Montesano *et al* (2014), who investigated spatially explicit aboveground biomass across a region of boreal forest transition using satellite laser altimetry complemented by high resolution spaceborne imagery. Their findings suggest a limited scope for accurately discerning gradients across the TTE using these data, as decreasing biomass is associated with unsuitably large increases in error terms. A different methodology based on MODIS vegetation continuous fields (VCFs) yielded similar results, as results suggested it to be unsuitable for differentiating between areas of less than 20% tree cover (Montesano *et al*, 2009). Although the success of these methods has thus far been limited, the considerable potential of remote sensing continues to drive research into its application.

Phenological methods based on variation in the seasonal characteristics of vegetation have also been used to research the TTE. Beck *et al* (2011) used NDVI fields to extract growing season length from satellite imagery, which was compared to gross productivity values derived from tree rings in North America for the period 1982-1991. The results support previous assertions that a biome shift has already begun along regions of the TTE, and suggest that the predicted increases in temperatures will make this transitional ecotone increasingly suitable for enhanced tree recruitment, leading to forest expansion. However they suggest that rates of climatic amelioration at the northern extent of the taiga will outpace tree recruitment potential, and that this will combine with losses at the southern extents of the boreal forest to result in a net decrease in forest area over the 21$^{st}$ century. Whilst not directly relevant to the present study of the TTE at the northern extents of the taiga biome, this provides important context for consideration of the overall future of the boreal forests.

Park *et al* (2016) used phenological data from a 33-year period between 1982 and 2014, in the form of NDVI summed over the full length of the growing season. Greening trends were found over 42.0% of northern vegetated areas, compared to browning over just 2.5% of the region. This was associated with significant advances in the start of the growing season and

delays to the end of the growing season, resulting in an overall lengthening of the season – a trend which was more pronounced over the Eurasian continent than the North American continent. This publication provides further support for the significant impact that climate change is having on high latitude vegetation.

One limitation in ongoing TTE research is that whilst some methods of mapping the ecotone have been successful, the time series of available data is not yet long enough to facilitate the repeat mapping which would allow temporal changes in vegetation ranges to be detected. For example, Ranson *et al* (2011) mapped the circumpolar TTE using VCFs for a single time period using a methodology that successfully represented high latitude vegetation variation. Although this methodology shows some promise for repeated use in the future to create comparative maps, the spatially coarse nature of the data used (2.5 km VCF pixel size) means it is uncertain whether crucial decadal scale changes in vegetation could be suitably captured using this methodology. The utility in the short term is therefore inconclusive. Such results informed the research of Montesano *et al* (2016), who considered the use of Landsat data at a 30 m spatial resolution as the input to a calibrated, domain-specific model of tree cover canopy, with results suggesting improvements to the reliability of ecotone characterization using this method. This is some of the most recent, and most promising, published work into methods of researching the TTE.

### What is the research gap that the present study is aiming to fulfil?

A clear factor from the reported research is that different studies use different variables to quantify variation in the TTE, and none has yet been proven superior to the others. Various studies use tree canopy cover, crown closure, growing season length and summed NDVI values to investigate vegetation change (Hadi *et al*, 2016; Montesano *et al*, 2016; Park *et al*, 2016; Ranson *et al*, 2011; Beck *et al*, 2011; Kharuk *et al*, 2007). Tree canopy cover is regularly used as it can be extracted from VCFs, and is robust to changes in the spatial resolution of data, making it suitable for use in comparative studies of different remote sensing platforms (Sexton *et al*, 2013). By contrast, accurate quantification of crown closure requires data with a relatively high spatial resolution, and so this vegetation parameter cannot be used in research based on low spatial resolution satellite data (Ranson *et al*, 2004). NDVI is applied to vegetation studies globally, over a variety of spatial and temporal scales, and is commonly used in phenological studies. It shares the benefit of tree canopy cover that it can be applied successfully to data sources with a variety of spatial resolutions.

The potential of phenology for investigating the TTE has been shown by a number of authors (Park *et al*, 2016; Beck *et al*, 2011). Beck *et al* (2007) assert that understanding

phenology is particularly important to climatically themed research as the timings of phenological events are primary responses to climate change at the ecosystem level. However the scope of previous phenological studies is limited to consideration of basic phenological parameters – notably growing season length and greenness (USGS, 2015). This is fairly common in phenological studies. Whilst these parameters provide valuable insight into certain aspects of vegetation seasonality, they fail to capture the full complexity of phenological characteristics. Notably, they do not suitably account for how vegetation changes between the start and end of season dates, particularly considering rates of change. An aim of this study is to construct a data analysis method which more effectively utilises a range of phenological data, in order to further explore the potential of using phenology to differentiate between vegetation types.

The application of annual phenological profiles for investigating high latitude vegetation is a novel approach, having only recently been explored by Daffern (2017). This pilot study demonstrated that MODIS NDVI data showed significant differences between annual phenology for disperse sites of tundra and taiga vegetation, suggesting the viability of the research method and prompting the need for further research into its application. However the scope was limited in terms of the number of sites used (six per biome, distributed throughout the northern hemisphere), the time period for which data was retrieved (the single calendar year of 2016) and the number of images used to create the time series of NDVI values representing site phenology (23 images per site). A major flaw in the previous study was the lack of consideration of vegetation index quality assurance data, leading to errant results in non-summer months which did not represent variation in vegetation. The limitations of the previous study are used to inform methodological improvements for the present study.

NDVI is a unitless parameter used to indicate vegetation greenness (Equation 1). It is chosen for use in constructing phenological profiles for two main reasons. Primarily, NDVI is widely used in phenological studies due to its value for discriminating seasonal vegetation changes linked to greenness controlled by leaf chlorophyll content. This is a good indicator of vegetation variation as leaf chlorophyll content is linked to photosynthetic activity, which controls plant productivity. The ease of use associated with NDVI data is the second important motivation, as pre-processed NDVI scenes are available for large volumes of MODIS data, with quality assurance parameters alongside (NASA LP DAAC, 2016). This is a major benefit as it means that any methods developed using this data could be re-applied to new locations and/or time frames without requiring additional pre-processing of imagery, which could be computationally intensive and time consuming. Although Landsat imagery will not be used in the present study, automated processing of this data to NDVI is also available. Therefore if the developed methodology proves successful, it could be readily transferred to a complementary

remote sensing dataset – this directly links to the aforementioned benefit that NDVI can be applied to data sources with varying spatial resolutions, as Landsat data is produced with a nominal pixel size of 30 m, compared to the 250 m pixels of MODIS vegetation products.

$$NDVI = \frac{Near\ infrared - Red}{Near\ infrared + Red} \qquad \text{[Eq. 1]}$$

Some limitations of using NDVI include the facts that: (i) it is a 2D field parameter which fails to capture 3D variation in vegetation height and structure, sources of significant difference between tundra and taiga vegetation types; (ii) the index becomes saturated at high values, which is a particular concern when considering forested areas such as the taiga biome; and (iii) the presence of snow and cloud prevents data acquisition for surface vegetation, limiting the usefulness of the index in high latitude areas to relatively short snow-free periods during the summer months. Although these limitations do not eliminate the usefulness of the index for application to phenological studies, consideration of their impact is necessary in assessing the results of methods employing NDVI.

## 1.2 Aims and Objectives

The aim of this work is to investigate the extent to which high latitude vegetation on the Kola Peninsula can be differentiated using NDVI-based phenology extracted from multispectral satellite imagery. The primary data source for this study will be MODIS, providing moderate spatial resolution imagery with a moderately high temporal resolution. The vegetation types under investigation include the Arctic tundra and taiga biomes, and the tundra-taiga ecotone which forms the transitional zone between the two. The presence of latitudinal, altitudinal and anthropogenic vegetation gradients for investigation using the novel phenological methodology make the Kola Peninsula in Western Russia a suitably interesting study site.

The primary aim will be achieved through the following objectives:

1. Extract NDVI data from time series of satellite imagery at sites representing various latitudinal, altitudinal and anthropogenic vegetation gradients.
2. Construct annual time series of phenological variability based on multi-year NDVI data.
3. Analyse whether significant differences exist between the phenological profile characteristics of transects representing various Arctic biomes and vegetation gradients.
4. Assess whether the results gained suggest that the methodology developed to investigate phenology could usefully be used to differentiate high latitude vegetation, considering the nature of any significant differences found to exist within or between the data sets.

Three key questions will form the focus of phenological profile analysis, in order to aid efforts to quantitatively differentiate the vegetation types associated with the tundra and taiga biomes:

1. How green does the vegetation get?
2. When does the vegetation start to get green?
3. At what rate does the greening process occur?

## 2 – Study Area

The study area for this research is the Kola Peninsula. The Western Russian peninsula lies between latitudes of 66.0˚ and 70.0˚, and spans longitudes of 30.0˚ to 42.0˚, with a total area of around 145,000 $km^2$ (Figure 1; Marshall *et al*, 2016). To its south is the White Sea, and to its north the Barents Sea. Houghton *et al* (2007) classify the region as belonging to the northern taiga/tundra zone, with vegetation on the peninsula ranging from major boreal forest stands to shrub tundra. The most prevalent taiga species are *Picea* spp., *Pinus* spp. and *Betula* spp. (Kozlov and Berlina, 2002; Saich *et al*, 2001; Gervais and MacDonald, 2001). Tundra species are more numerous, including dwarf shrubs such as *Vaccinium* spp. as well as *Sphagnum* mosses and lichens (Kravtsova and Loshkareva, 2013; Orlova *et al*, 2013).

Large areas of the peninsula form a part of the transitional TTE zone, which broadly follows the orientation of the northern coast from north-west to south-east. Tundra dominates along the northern coast of the peninsula associated with low-lying coastal regions, whilst taiga is prominent in the south (Virtanen *et al*, 2016; Blinova and Chmielewski, 2015; MacDonald *et al*, 2008; Koroleva, 1994). Local complexities in vegetation distribution are introduced due to altitudinal gradients, particularly around the Khibiny massif in the centre of the peninsula, and anthropogenic factors, especially linked to industrialization around the major cities of Murmansk and Monchegorsk in the west (Kremenetski *et al*, 1999; Saich *et al*, 2001; Vlassova, 2002). The terrain of the peninsula has a high roughness, with microtopography strongly influencing the heterogeneity of tundra vegetation, creating mosaics of various plant functional types (Chernon'kova *et al*, 2013; Kravtsova and Loshkareva, 2013; Koroleva, 1994). Surface water forms a significant aspect of the land cover on the peninsula, with mires a prevalent feature to the north and east, and abundant lakes throughout the region occupying bedrock depressions formed beneath the Scandinavian ice sheet (Blinova and Chmielewski, 2015; Gervais and MacDonald, 2002). Elevation across the Kola Peninsula is mapped in Figure 2, based on GMTED2010 data (USGS, 2010).

A 50-year study of the climate of the Kola Peninsula conducted by Marshall *et al* (2016) shows an average surface air temperature of ~0˚C, with positive values more likely to occur coastally due to the moderating effect of the ocean. Annual surface air temperatures showed a positive trend of 2.3˚C ± 1˚C over the 50 year period 1966-2015. The same study shows average annual precipitation ranging from ~600 mm to ~430 mm, decreasing from west to east due to the influence of the North Atlantic Current in the Barents Sea. A shift in seasonality to wetter springs and drier autumns is reported over the same time period. The snow-free season usually extends from June until mid-October, though this is locally variable depending on relief and aspect (Koroleva, 1994). Beck *et al* (2007) show that the onset of spring across the peninsula

varies between late May and mid June, with areas along the northern coast systematically later than those inland, which are in turn later than areas along the southern coast. Blinova and Chmielewski (2015) found high heterogeneity in the regional climate for the Kola Peninsula, suggesting subdivision based on the relative influences of latitude, longitude, altitude, oceanicity versus continentality and the extent of the Gulf Stream impact – many of which are inter-related (Gervais *et al*, 2002).

Eight transects for study have been selected across the Kola Peninsula, and are defined in terms of the MODIS pixels which represent them (Table 1; Figure 3). Each MODIS pixel has a nominal size of 250 m. Six of the eight transects are each 50 pixels long by 10 pixels wide (nominally 12.5 km by 0.25 km), and include five sites, each with a length of 10 pixels. Four of these transects characterize areas of known tundra or taiga vegetation coverage, with two north-south oriented transects selected per biome. Each tundra transect (T1 & T2) is paired with a taiga transect (F1 & F2) of approximately the same longitude; both tundra transects lie considerably north of the associated taiga transect. The other two short transects represent special cases of smaller-scale vegetation transition. One is located near the city of Monchegorsk (M), allowing investigation of a technogenic gradient related to anthropogenic impacts along an east-west axis, and the other spans the northern flank of the Khibiny Mountains (K), allowing investigation of altitudinal vegetation change along a north-south axis. The Monchegorsk site was selected based on the vegetation maps created by Shipigina and Rees (2012) using trained classification of remotely sensed imagery at a high spatial resolution; all other sites were selected with reference to the vegetation maps of Blinova and Chmielewski (2015) and Schwartz and Reed (1999) shown in Figure 4 an dFigure 5. Two large transects have been created to investigate broader regional-scale vegetation changes; these transects will act as test locations for the differentiation of vegetation based on the results of the tundra and taiga transects. One is oriented approximately east-west, and will be referred to as the longitudinal transect (X), and the other north-south, to be known as the latitudinal transect (Y). Each of these transects is 1000 pixels long by 10 pixels wide (250 km by 0.25 km). The two longer transects are each divided into 25 sites, each with a length of 40 pixels (10 km).

Figure 1: Map showing the location of the Kola Peninsula in European Russia, to the east of Norway and Finland. Produced using NaturalEarth data.

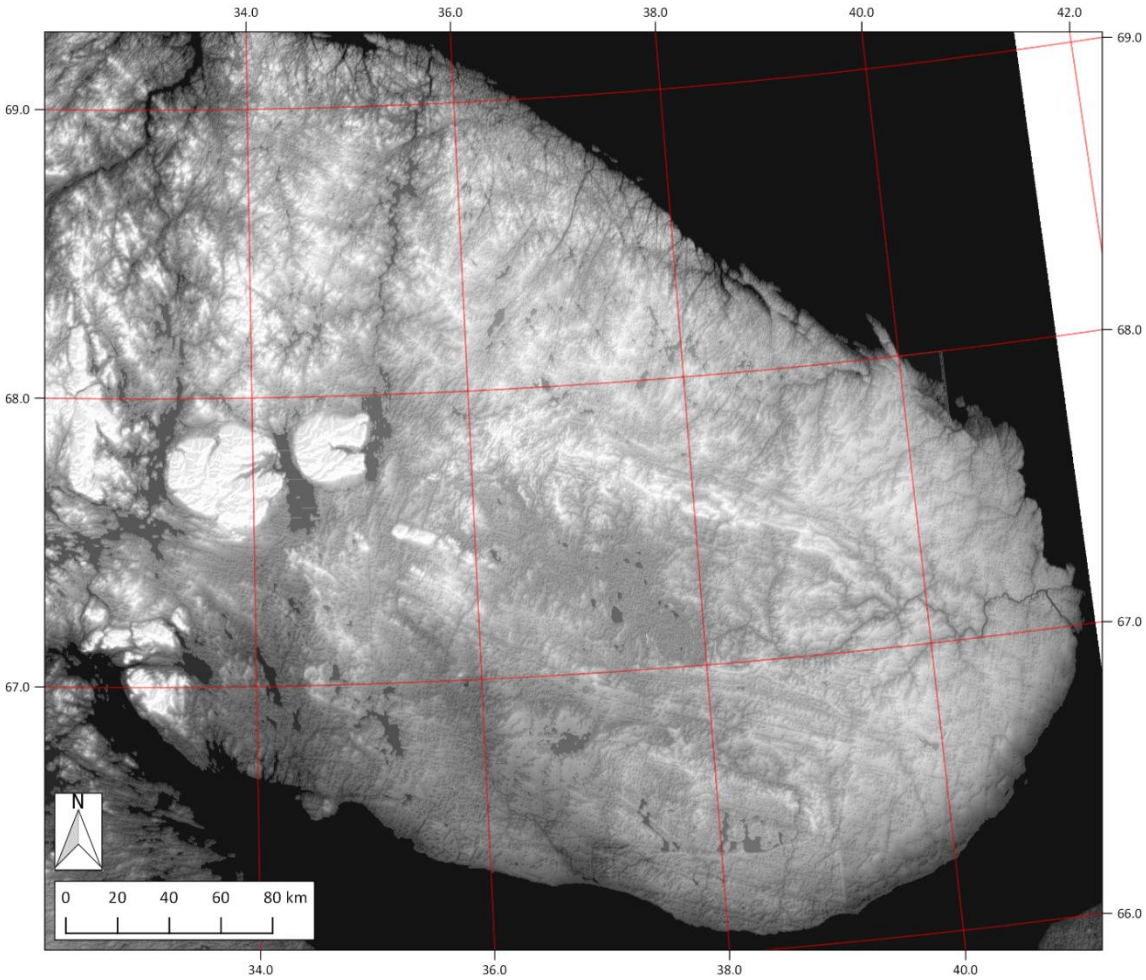


Figure 2: Map showing elevation across the Kola Peninsula. Lighter shades represent areas of greater elevation. Produced using GMTED2010 DEM data (USGS, 2010).

| Transect Name | Identifier | Lower X | Upper X | Lower Y | Upper Y | Orientation |
|---|---|---|---|---|---|---|
| Tundra 1 | T1 | 662515.0593 | 664831.6229 | 7603889.743 | 7615472.561 | North-south |
| Tundra 2 | T2 | 624291.7602 | 626608.3238 | 7583040.671 | 7594623.489 | North-south |
| Taiga 1 | F1 | 662515.0593 | 664831.6229 | 7380341.357 | 7391924.175 | North-south |
| Taiga 2 | F2 | 624291.7602 | 626608.3238 | 7435938.883 | 7447521.701 | North-south |
| Monchegorsk | M | 489931.0724 | 501513.8903 | 7525126.581 | 7527443.145 | West-east |
| Khibiny | K | 533945.7805 | 536262.3441 | 7522810.018 | 7534392.836 | North-south |
| Longitudinal | X | 467692.062 | 699348.4203 | 7590222.018 | 7592538.582 | West-east |
| Latitudinal | Y | 753787.6645 | 756104.228 | 7342349.715 | 7574006.073 | North-south |

Table 1: Transect information. XY coordinates are given in transverse Mercator meters for UTM Zone 36N.

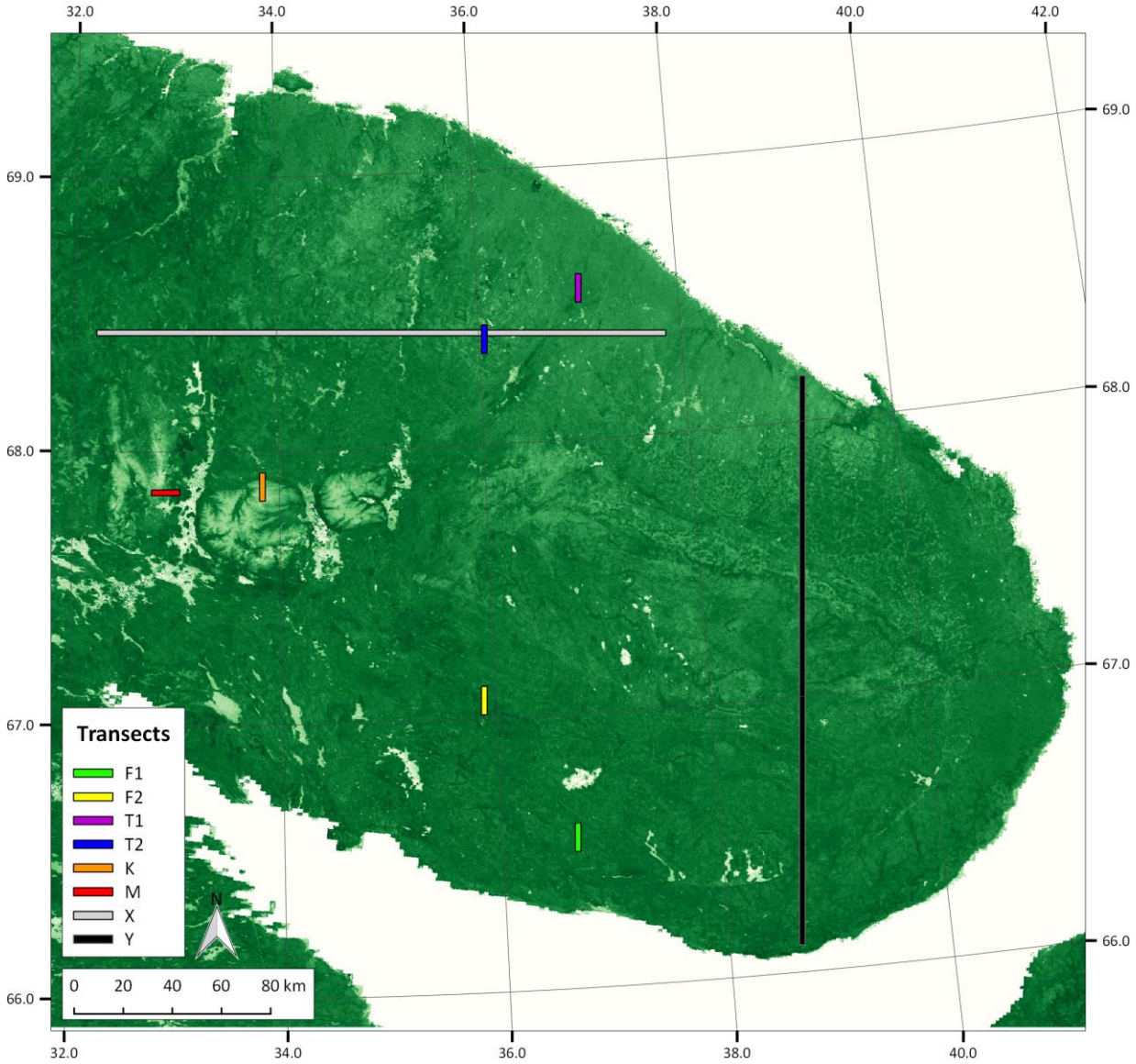


Figure 3: Map showing transect locations across the Kola Peninsula. The background image is the MOD13Q1 scene for Julian Day 193, 2016, pseudo-colourised on a ramped green scale with darker shades representing greater NDVI values.

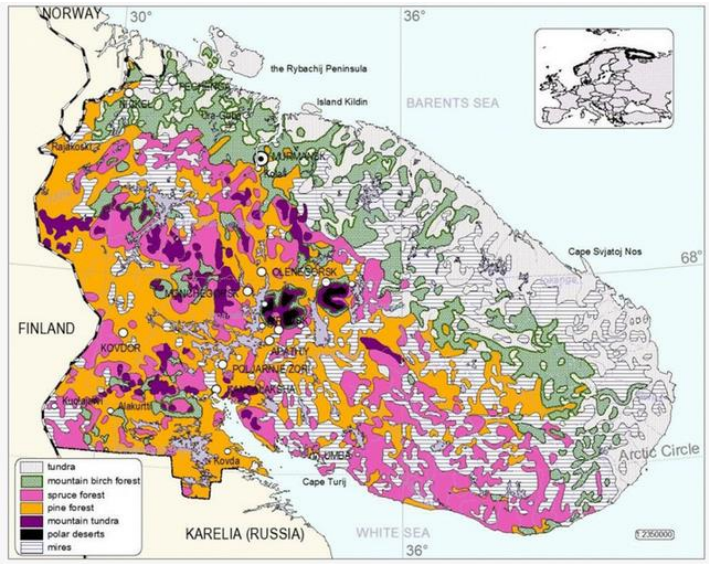


Figure 4: Map of Murmansk region vegetation, including the Kola Peninsula, based on 1971 data. Source: Blinova and Chmielewski, 2015.

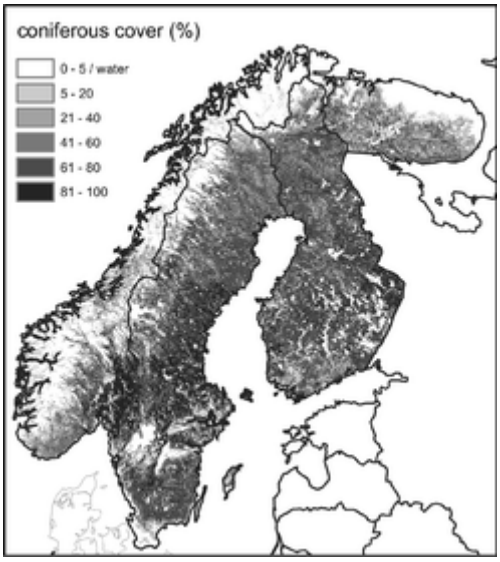


Figure 5: Map of coniferous forest in northern Scandinavia, based on NOAA AVHRR data. Source: Schwartz and Reed, 1999.

# 3 – Methods

MODIS imagery MOD13Q1 and MYD13Q1 are downloaded via the EarthExplorer website using the Bulk Download Application tool. Scenes are acquired in HDF-EOS format. Each scene is a mosaic constructed of pixels representing the best quality remotely sensed data for a 16-day period. For MOD13Q1 these 16-day periods begin on Julian Day (DOY) 001 each year, whilst for MYD13Q1 the image periods begin on DOY 009. The 8-day offset allows better temporal coverage of the Earth's surface to be provided. However the stated dates must be treated with some cynicism, as the pixels used to construct the final mosaic could be from images acquired on any date within the 16-day period. It is therefore possible that for any selection of a consecutive MOD and MYD image pair, the order in which the images are given may not reflect the order in which the pixels are recorded. For example, pixels included in a MYD scene beginning on DOY 009 may reflect an earlier surface state than those included in a MOD scene beginning on DOY 001, if the best quality MYD pixels are gathered on DOY 011 and the best quality MOD pixels are gathered on DOY 015. The discrete, 8-day nature of the data acquired from MODIS results in some temporal limitations to the research conducted herein, with uncertainties present in the accuracy of the DOY designations.

The MOD13Q1 data series begins on 18.02.2000 whilst the MYD13Q1 data series begins on 04.07.2002. The period of this study therefore begins in February 2000, with data availability doubling from July 2002. All scenes from both data sets are used in full from the start of data collection until the final scene of 2016, on DOY 353 for MOD13Q1, and DOY 361 for MYD13Q1. Each time series contains 23 scenes per year, meaning that a total of 388 MOD scenes and 334 MYD scenes are available for analysis over the given time period. The full study area is contained within tile h = 19, v = 2 of the sinusoidal projection for which the MODIS land products are produced. Data is provided with a nominal spatial resolution (pixel size) of 250 m.

Downloaded scenes are processed using the MODIS Reprojection Tool (NASA LP DAAC, 2011). Only the Normalized Difference Vegetation Index (NDVI) and Vegetation Index Quality (VI_Quality) layers are retained during processing. Each image is spatially subset to contain the Kola Peninsula and immediately surrounding areas, with the upper left coordinate at (69.663319, 31.025639) and the lower right coordinate at (65.888014, 41.233563). Nearest neighbour resampling is used to reproject each image to the Universal Transverse Mercator (UTM) projection for zone 36N.

Image analysis is undertaken in the MATLAB programming environment (MathWorks, 2015). Individual transects are isolated based on absolute pixel values with reference to the top left corner of the scene, and are then converted to geographical locations based on transverse Mercator meters. This methodology is robust due to the images having previously been cropped

to precisely the same geographical area. Transect positions are chosen with reference to the MOD44W water mask, to minimise the inclusion of major water bodies (NASA LP DAAC, 2014).

For each pixel within each site of each image, the 16-bit value of the associated VI_Quality pixel is considered. If the quality assurance suggests that the VI pixel was produced with good quality (bits 0-1 == 00), the associated pixel in the main NDVI image is included in further analysis. All other pixels are removed. Sites are considered valid for use if a 50% threshold of good quality pixels is met or exceeded. At each site where these conditions are met, NDVI average is calculated based only on the retained good quality pixels. For each site the median of all available mean values for each DOY is found, and an annual phenological profile is constructed based on a time series of these medians.

Quantitative analysis of this annual phenological profile is undertaken to parameterize key phenological features for comparison between sites. For each site, seven key parameters are identified, as shown in Table 2. In all cases, missing data points are excluded from the analysis. The end of winter (P1) and start of summer (P2) dates are the main input allowing for further analysis, and are identified manually prior to the calculation of the other parameters. The end of winter date indicates the last day preceding the pronounced increase in NDVI values associated with spring greening of vegetation. The start of summer date marks the end of this rapid increase. These points are readily identifiable in the majority of profiles; identification is only ambiguous for a small number of sites, mostly localised to the Monchegorsk transect.

The mean winter NDVI (P3) is calculated as the average of all NDVI values up to and including the end of winter date. The spring NDVI rate of change (P4) is calculated as the gradient of the linear fit between the end of winter and start of summer data points, and is given in units NDVI per day. Data points from the start of summer until the end of the time series are all considered to represent summer, as the time series systematically end during late September or early October, due to a lack of good quality data available later in the year. A second order polynomial is fit to the summer data to approximate the changing NDVI profile. The turning point of the polynomial is evaluated to identify the day of the year when maximum NDVI is reached (P5). This date is used as input for the polynomial to calculate the value of the maximum NDVI (P6). The summer trendline curvature (P7) is the coefficient of the quadratic term, which represents the rate of NDVI change throughout the summer season. Plots are created for each site showing the annual phenological profile of medians, with the summer polynomial overlaid.

A number of variables are calculated based on these parameters in order to further quantify phenology. The length of spring is found by calculating the difference between the start of summer and the end of winter dates (P2 – P1). In order to assess the level of agreement between P5 and the actual date of measured maximum NDVI, and P6 and the measured

maximum NDVI, the value of each of the two parameters is subtracted from the associated measured value to produce residuals. Positive residuals suggest an underestimation of the measured value by the parameter; negative residuals indicate an overestimation. For the tundra and taiga transects, averages of each parameter from P3 to P7 is found, in order to test the possibility of establishing baseline variables for each of the biome vegetation types. Means are also found for the residuals related to P5 and P6, in order to investigate whether any systematic errors exist between these parameters and the measured values they are intended to represent. Based on the parameterization results, parameter ranges representing tundra and taiga vegetation are found, with those which fall into areas of overlap defined as ambiguous. These ranges are conditionally applied to the parameterization results of the longitudinal and latitudinal transects in order to attempt biomization of their constituent sites based on classification of the ground cover, and thus empirically test the utility of the tundra and taiga results for differentiating between vegetation types across a broader geographical range.

| Identifier | Parameter |
|---|---|
| P1 | End of Winter Date |
| P2 | Start of Summer Date |
| P3 | Mean Winter NDVI |
| P4 | Spring NDVI Rate of Change |
| P5 | Maximum NDVI Date |
| P6 | Maximum NDVI (at P5) |
| P7 | Summer Trendline Curvature |

Table 2: Phenological parameter identification.

# 4 – Results

The full parameterization results for the tundra, taiga, Khibiny and Monchegorsk transects which are referred to in the next four sections are presented in Table 3. Table 4 provides the calculated values of difference between the measured dates of maximum NDVI, the measured values of maximum NDVI, and the associated calculated parameters P5 and P6 for the six short transects.

## 4.1 Tundra Transects, T1 & T2

The vegetation at sites within the tundra transects demonstrate similar phenological profile characteristics. Figure 6 shows an example profile for site T1.1. Tundra sites consistently have P3 values below zero, averaging -0.0403, with NDVI only becoming positive during the spring greening period. P1 varies between DOY 121 and DOY 137, with a direct correlation between increasing latitude and later end of winter dates. Only the southernmost site has EOW on DOY 121; the two next southernmost sites have EOW on DOY 129, with the EOW occurring on DOY 137 at the remaining seven tundra sites. P2 dates range from DOY 137 to DOY 153. Of the six southernmost sites, five have SOS dates of 145 and one has a SOS date of 137. The four northernmost sites all have SOS dates of 153.

The length of spring varies between 8 days and 24 days for tundra sites. Four of the five sites in T1 have a 16-day spring period, with only the southernmost having an 8-day spring. Three of the five sites in T2 have 8-day spring periods. Only the southernmost site of the T2 transect has a 24-day spring period, due to this site having the earliest EOW of any of the sites combined with a SOS date in line with the majority of the sites within the same transect. P4 varies between 0.001113 and 0.002253 across all tundra sites, with an average of 0.001520. Both the highest and the lowest gradients are present in T1, which has a mean of 0.001511, marginally lower than the T2 average of 0.001529.

P5 varies between DOY 210 and DOY 215 to the nearest full day for tundra sites, with an average of DOY 213. Measured NDVI values reach their maximum on DOY 201 for all tundra sites. The parameterization therefore consistently overestimates the DOY when maximum NDVI is reached compared to the actual values (Table 4). This varies by between 9 and 14 days, with an average overestimation of 12 days. This overestimation effect is more pronounced for the T1 transect than the T2 transect.

In contrast, the parameterization consistently underestimates P6 in comparison to measured maximum NDVI values. P6 varies between 0.65570 and 0.72266 with a mean of 0.68630. Actual values range from 0.67197 and 0.74255, with a mean of 0.70660. This is

reflected in the fact that the average underestimation by P6 is 0.02030. This underestimation is more pronounced in T2, averaging 0.02343, compared to the T1 transect average of 0.01717.

P7 showed that the curvature of the summer trendline decreased with increasing latitude within T1, but showed no trend within T2. Across all sites within the tundra transects, T1 contained both the greatest curvature of -4.97E-05 at T1.5, and the least curvature of -3.63E-05 at T1.1. The average P7 across tundra sites was -4.26E-05. Tundra data was available for all sites until DOY 281, after which no usable data was available. This suggests a summer growing season lasting between 128 and 144 days.

In summary, tundra profiles are typified by winter NDVI values below zero, which begin to rise between DOY 129 and DOY 137. This rapid increase represents a spring period usually between 8 and 16 days in length, with NDVI rising by 0.001520 per day on average. Maximum summer NDVI was consistently reached on DOY 201, with an average value of 0.68630. Parameterization systematically overestimates P5 and underestimates P6 for sites within the tundra transects. The average curvature of the second-order polynomial fit to the tundra summer NDVI data is -4.26E-05, across a summer season of approximately 4.5 months between late May and early October.

### 4.2 Taiga Transects, F1 & F2

The phenological profiles of taiga transect vegetation demonstrate similar characteristics. Figure 7 shows an example profile for site F1.1. For the taiga transects P3 is consistently above zero, with an average of 0.0241. P3 increases with decreasing latitude for F2; no trend is present in this variable for F1. P1 and P2 are consistent across all taiga sites, with the former occurring on DOY 121 and the latter on DOY 129. The spring period is always 8 days in length. P4 varies between 0.001927 and 0.002643, with an average of 0.002192. The transect averages are 0.002188 and 0.002196 for F1 and F2 respectively.

P5 values range from DOY 204 to DOY 208 for taiga sites. The mean value across all sites is around DOY 206. The P5 average is 207 for F1, two days later than the 205 average for F2. Measured values of NDVI are at a maximum on DOY 201 for the majority of taiga sites, with only two sites showing maximum values slightly earlier on DOY 193. The parameterization overestimates P5 by approximately 8 days for F1 and 6 days for F2. These values are skewed by the two sites F1.5 and F2.3, which have maximum NDVI occurring on DOY 193. The errors for these sites are close to 15 and 13 days each, which increases the average overestimation by approximately 1.5 to 2 days compared to the eight other sites.

P6 values range from 0.72650 to 0.78769, with an average of 0.76841 across all sites. F1 has slightly lower associated P6 values than F2, with a difference in means of 0.00565. P6

consistently underestimates the maximum NDVI in comparison to the measured values. The average difference between P6 and the actual maximum value is 0.01470, with variation between 0.01067 and 0.01745 for individual sites. The spatial variation in P6 is shown for all transects in Figure 8.

P7 values vary significantly between F1 and F2. The overall average is -3.95E-05. However the average curvature of the summer trendline was -3.69E-05 for F1, which is noticeably less pronounced than the -4.21E-05 average curvature for F2. Neither transect showed consistent latitudinal trends in P7 – however the greatest curvature of -4.72E-05 occurred for F2.2, the second most northern site, and the least curvature of -3.19E-05 was present in F1.5, the furthest south of the taiga sites. The length of the summer season for taiga sites was 152 days for all sites due to the consistency between the SOS on DOY 209, and the end of the useable data record on DOY 281 throughout both transects.

In summary, taiga profiles are characterised by winter NDVI values slightly above zero, which begin to rise on DOY 121. The rapid spring increase occurs over a period of 8 days, with an average increase in NDVI of 0.002192 per day. Maximum summer NDVI is reached on DOY 193 or 201, and has a mean value of 0.76841. On average, parameterization of taiga phenological profiles overestimates P5 by approximately 7 days, and underestimates P6 by 0.01470. The average curvature of the summer NDVI trend is -3.95E-05, though this shows considerable variation of 5.19E-06 between the two taiga transects. The length of the summer season is approximately 5 months, beginning in early May and terminating in early October.

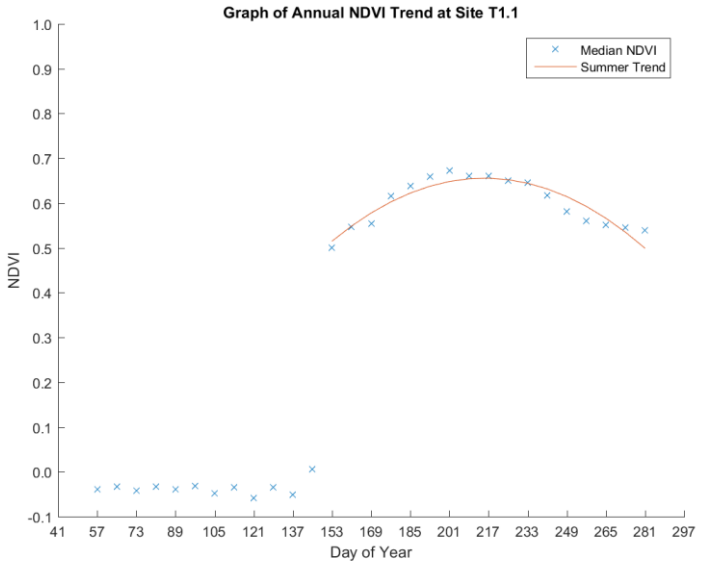


Figure 6: Graph showing a typical annual phenological profile for a tundra site.

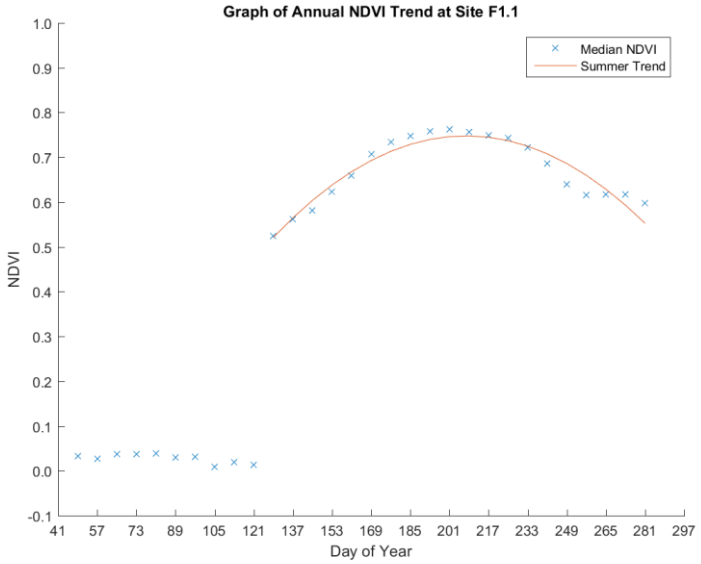


Figure 7: Graph showing a typical annual phenological profile for a taiga site.

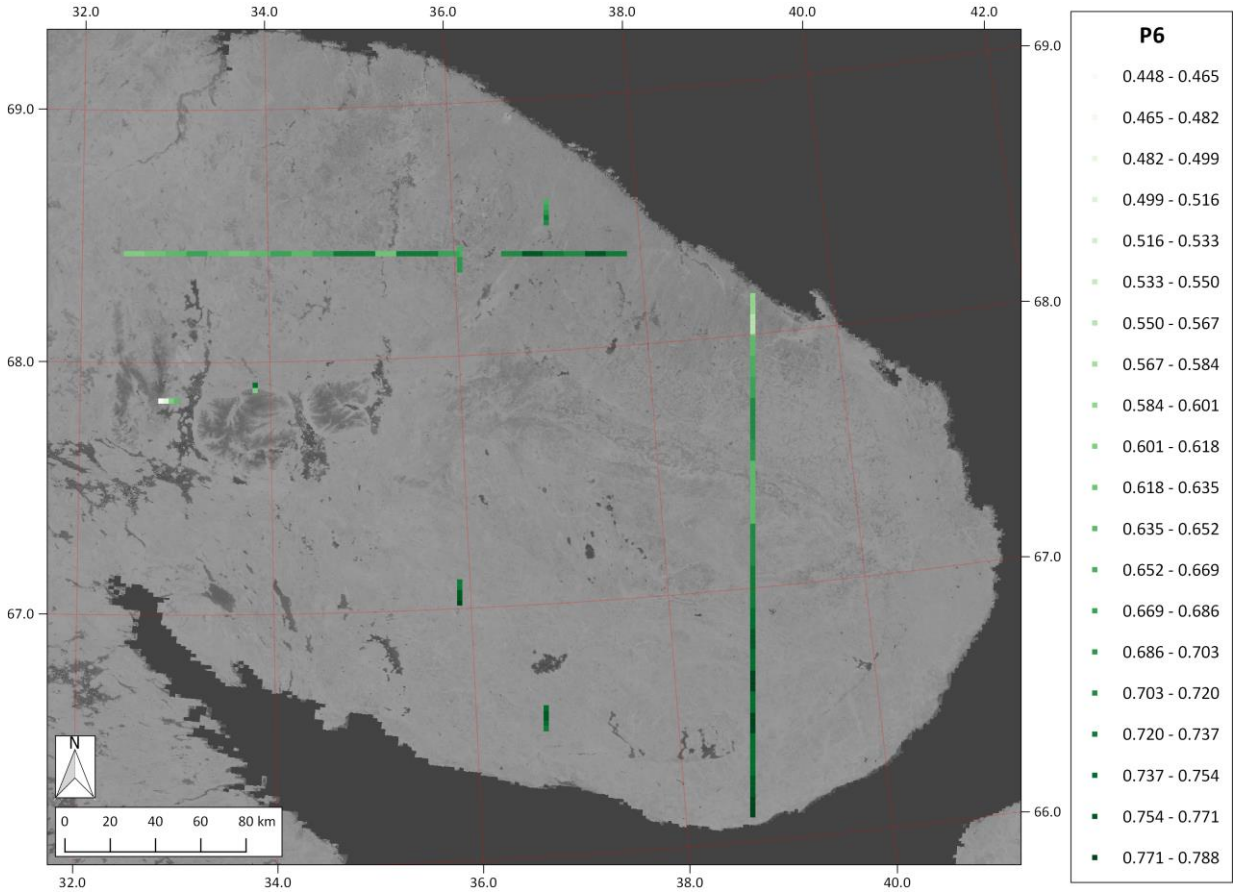


Figure 8: Map showing geographical variation in P6 across all transects.

### 4.3 Khibiny Transect, K

Of the five sites within the Khibiny transect, only sites K.1 and K.2 produced sufficient NDVI data for the parameterization procedure to be undertaken. Sites K.4 and K.5 provided only a limited number of winter data points. Site K.3 provided a number of data points throughout winter and summer, however key dates containing the spring greening period were missing any usable data. Decreasing availability of data points is directly correlated to increasing altitude within the massif. Significant differences exist in the parameterization results of the two Khibiny sites providing sufficient data for analysis.

The phenological profiles for sites K.1 and K.2 are shown in Figure 9. The P1 values of sites K.1 and K.2 are DOY 121 and DOY 129 respectively; both sites have P2 values of 137. Spring is therefore 8 days shorter at K.2 than at K.1, though the discrete nature of the measured Julian days means that there is an error of ±8 days associated with this value. P3 for K.2 is slightly negative at -0.0151, whereas P3 for K.1 is strongly positive at 0.1870. The winter NDVI variation at K.1 is strongly anomalous compared to all other sites used in this study, exhibiting a negative trend between DOY 57 and DOY 121, between which times all NDVI values are above 0.1. No other time series contains any winter NDVI values exceeding 0.1. The P4 value for K.1 is 0.002791, slightly higher than the value of 0.002191 for K.2.

P5 values for the Khibiny sites are DOY 218 and DOY 204 for K.1 and K.2 respectively, with associated P6 values of 0.74449 and 0.60628. Measured values show maximum NDVI occurring on DOY 201 for both sites, suggesting overestimations of 17 and 3 days for the two sites. These errors lie outside of the ranges observed for all sites within both the tundra and taiga transects. P6 values underestimate the actual maximum NDVI values reached by 0.02782 for K.1 and 0.01874 for K.2, however this degree of error is not unexpected based on analysis of the tundra and taiga transects. The P7 values associated with the K sites show very low degrees of curvature at -1.65E-05 and -2.01E-05 respectively. DOY 281 provided the last usable data for site K.1, giving a summer season length of 144 days, whereas the K.2 record ended on DOY 273, with a shorter summer season lasting 136 days.

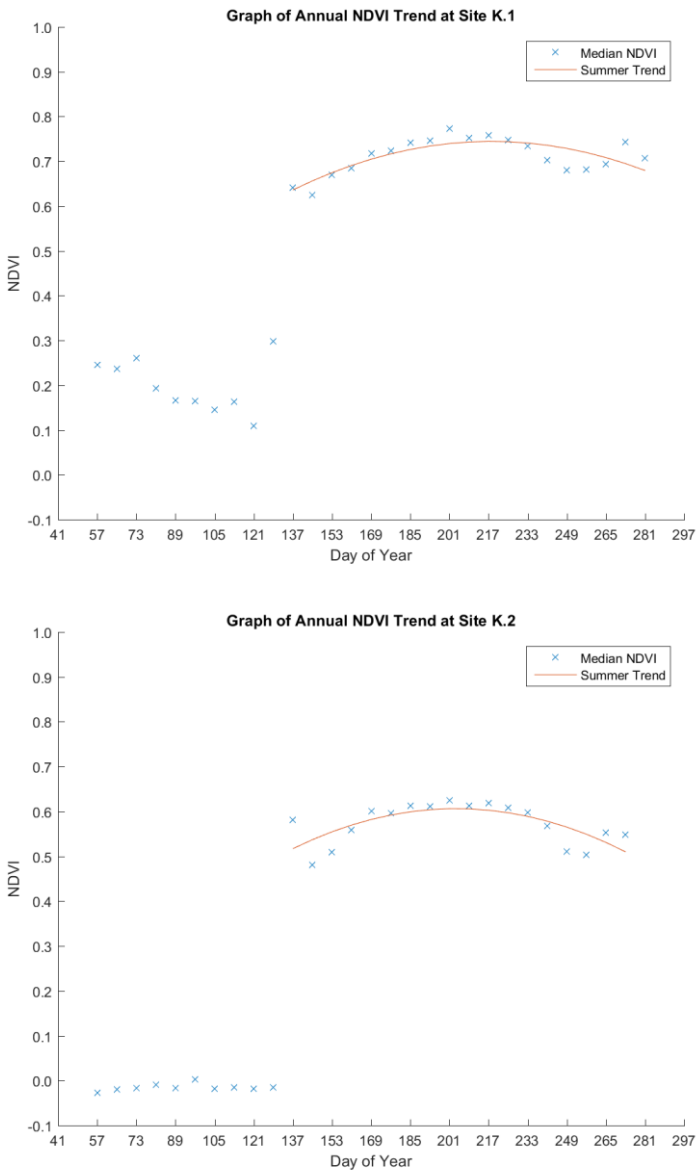


Figure 9: Graphs showing the annual phenological profiles for sites K.1 and K.2.

## 4.4 Monchegorsk Transect, M

Four of the five sites within the Monchegorsk transect provided sufficient data for parameterization to be undertaken, with only site M.1 necessarily excluded. Phenological profile graphs are shown for all four parameterized Monchegorsk sites in Figure 10. Alongside the forthcoming quantitative analysis, it is clear from qualitative analysis of these graphs that there is much greater variation between these phenological profiles than exists within the tundra and taiga sites. The strength of the distinctive features common to both the tundra and taiga sites – for example a distinct increase in NDVI during spring, and a fairly parabolic summer trend – are lacking from site M.2, and depressed for site M.3. The identification of the EOW and SOS dates was therefore less clear in these cases. In contrast, the phenological characteristics of sites M.4 and M.5 show good comparability to the profiles constructed from the tundra and taiga sites. Henceforth all quoted values for the Monchegorsk transect will be given in order from M.2 to M.5.

P1 values are 121 for M.2 and M.3, and 129 for M.4 and M.5; P2 values are 145 for M.2 and 137 for the M.3, M.4 and M.5. The length of spring therefore decreases from 24 days for M.2, to 16 days for M.3, to 8 days for M.4 and M.5. P3 was greatest for M.2 at 0.0348, and lowest for M.5 at -0.0091; the P3 values for M.3 and M.4 were similar, at 0.0077 and 0.0102 respectively. P4 values show no consistent trend, though the two greatest gradients are related to the sites with the shorter 8-day spring period.

P5 values for sites M.2 and M.3 are DOY 210 and DOY 202, both of which are major overestimations of 25 and 17 days compared to the actual value of DOY 185 on which the maximum NDVI is reached for both sites. In comparison the P5 values of M.4 and M.5 are 215 and 213; the former of these slightly underestimates the actual value by 2 days, whereas the latter is a 4-day overestimation.

P6 shows a consistent increase from site M.2 to site M.5, ranging from 0.44751 through 0.51373 and 0.60651 to 0.64672. Whilst all of the values are slight underestimations of the measured maximum NDVI, the error is more significant for M.2 and M.3 than for M.4 and M.5.

Similarly to P3, P7 does not show a consistent along-transect pattern, however the least significant curvature of -2.03E-05 is associated with M.2, whilst the most significant curvature of -3.34E-05 is associated with M.5. The summer trend of site M.3 has slightly greater curvature than that of site M.4. The time series of usable data ends on DOY 273 for all sites within the Monchegorsk transect, giving summer season lengths of 128 days for M.2, and 136 days for M.3, M.4 and M.5.

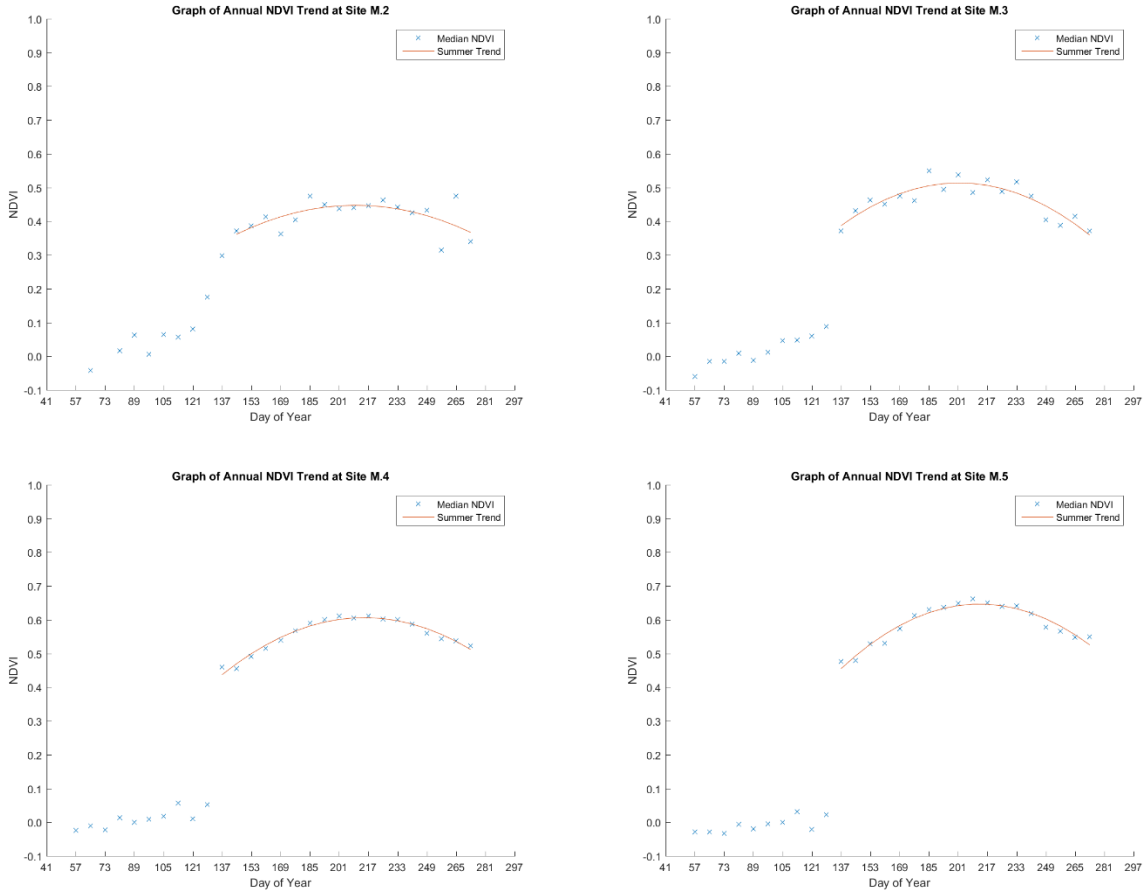


Figure 10: Graphs showing the annual phenological trends for sites M.2, M.3, M.4 and M.5.

| Transect | Site | P1 | P2 | P2-P1 | P3 | P4 | P5 | P6 | P7 |
|---|---|---|---|---|---|---|---|---|---|
| **T1** | **1** | 137 | 153 | 16 | -0.040395 | 0.001113 | 215.29 | 0.6557 | -3.63E-05 |
| | **2** | 137 | 153 | 16 | -0.036856 | 0.001226 | 215.49 | 0.68271 | -3.94E-05 |
| | **3** | 137 | 153 | 16 | -0.035969 | 0.001408 | 213.19 | 0.69782 | -4.03E-05 |
| | **4** | 137 | 153 | 16 | -0.038436 | 0.002253 | 210.32 | 0.72266 | -4.54E-05 |
| | **5** | 137 | 145 | 8 | -0.042073 | 0.001555 | 212.57 | 0.70516 | -4.97E-05 |
| **T2** | **1** | 137 | 145 | 8 | -0.045945 | 0.001524 | 214.62 | 0.66175 | -4.16E-05 |
| | **2** | 137 | 145 | 8 | -0.044904 | 0.001551 | 213.78 | 0.66416 | -4.22E-05 |
| | **3** | 129 | 145 | 16 | -0.040998 | 0.001363 | 212.37 | 0.69716 | -4.66E-05 |
| | **4** | 129 | 137 | 8 | -0.039461 | 0.001768 | 211.20 | 0.6862 | -4.10E-05 |
| | **5** | 121 | 145 | 24 | -0.037618 | 0.001438 | 211.63 | 0.68968 | -4.37E-05 |
| **F1** | **1** | 121 | 129 | 8 | 0.027383 | 0.002213 | 207.85 | 0.74797 | -3.65E-05 |
| | **2** | 121 | 129 | 8 | 0.021113 | 0.002188 | 206.81 | 0.75841 | -3.84E-05 |
| | **3** | 121 | 129 | 8 | 0.038374 | 0.002249 | 206.91 | 0.76734 | -4.01E-05 |
| | **4** | 121 | 129 | 8 | 0.0056685 | 0.002136 | 207.53 | 0.75123 | -3.77E-05 |
| | **5** | 121 | 129 | 8 | 0.0034668 | 0.002154 | 207.79 | 0.72945 | -3.19E-05 |
| **F2** | **1** | 121 | 129 | 8 | 0.0022111 | 0.001927 | 206.40 | 0.7265 | -4.33E-05 |
| | **2** | 121 | 129 | 8 | 0.0042801 | 0.001928 | 205.18 | 0.73586 | -4.72E-05 |
| | **3** | 121 | 129 | 8 | 0.026014 | 0.002264 | 205.84 | 0.76378 | -4.04E-05 |
| | **4** | 121 | 129 | 8 | 0.026926 | 0.002219 | 204.39 | 0.76884 | -4.31E-05 |
| | **5** | 121 | 129 | 8 | 0.086021 | 0.002643 | 204.68 | 0.78769 | -3.65E-05 |
| **K** | **1** | 121 | 137 | 16 | 0.18701 | 0.002791 | 218.15 | 0.74449 | -1.65E-05 |
| | **2** | 129 | 137 | 8 | -0.015118 | 0.002191 | 203.72 | 0.60628 | -2.01E-05 |
| | **3** | | | | | | | | |
| | **4** | | | | | | | | |
| | **5** | | | | | | | | |
| **M** | **1** | | | | | | | | |
| | **2** | 121 | 145 | 24 | 0.034763 | 0.001785 | 210.02 | 0.44751 | -2.03E-05 |
| | **3** | 121 | 137 | 16 | 0.0076973 | 0.001388 | 201.60 | 0.51373 | -3.03E-05 |
| | **4** | 129 | 137 | 8 | 0.010153 | 0.001968 | 214.84 | 0.60651 | -2.80E-05 |
| | **5** | 129 | 137 | 8 | -0.0090494 | 0.001923 | 212.76 | 0.64672 | -3.34E-05 |

Table 3: Full parameterization results for the tundra (T), taiga (F), Khibiny (K) and Monchegorsk (M) transects.

| Transect | Site | Date of Maximum NDVI | Date of Maximum NDVI - P5 | Maximum NDVI | Maximum NDVI - P6 |
|---|---|---|---|---|---|
| **T1** | **1** | 201 | -14.29 | 0.67197 | 0.01627 |
| | **2** | 201 | -14.49 | 0.70139 | 0.01868 |
| | **3** | 201 | -12.19 | 0.7157 | 0.01788 |
| | **4** | 201 | -9.32 | 0.74255 | 0.01989 |
| | **5** | 201 | -11.57 | 0.7183 | 0.01314 |
| **T2** | **1** | 201 | -13.62 | 0.68613 | 0.02438 |
| | **2** | 201 | -12.78 | 0.68125 | 0.01709 |
| | **3** | 201 | -11.37 | 0.71779 | 0.02063 |
| | **4** | 201 | -10.2 | 0.71645 | 0.03025 |
| | **5** | 201 | -10.63 | 0.71447 | 0.02479 |
| **F1** | **1** | 201 | -6.85 | 0.76208 | 0.01411 |
| | **2** | 201 | -5.81 | 0.77586 | 0.01745 |
| | **3** | 201 | -5.91 | 0.78443 | 0.01709 |
| | **4** | 201 | -6.53 | 0.7619 | 0.01067 |
| | **5** | 193 | -14.79 | 0.74141 | 0.01196 |
| **F2** | **1** | 201 | -5.4 | 0.73894 | 0.01244 |
| | **2** | 201 | -4.18 | 0.75253 | 0.01667 |
| | **3** | 193 | -12.84 | 0.77883 | 0.01505 |
| | **4** | 201 | -3.39 | 0.7836 | 0.01476 |
| | **5** | 201 | -3.68 | 0.80447 | 0.01678 |
| **K** | **1** | 201 | -17.15 | 0.77231 | 0.02782 |
| | **2** | 201 | -2.72 | 0.62502 | 0.01874 |
| | **3** | | | | |
| | **4** | | | | |
| | **5** | | | | |
| **M** | **1** | | | | |
| | **2** | 185 | -25.02 | 0.47534 | 0.02783 |
| | **3** | 185 | -16.6 | 0.54932 | 0.03559 |
| | **4** | 217 | 2.16 | 0.61131 | 0.0048 |
| | **5** | 209 | -3.76 | 0.66134 | 0.01462 |

Table 4: Comparison between measured variables and the associated parameters for the tundra, taiga, Khibiny and Monchegorsk transects. Positive values suggest an under-estimation during parameterization whilst negative values suggest an over-estimation.

### 4.5 Longitudinal Transect, X

Table 5 shows full parameterization results for the longitudinal transect. Three sites in the longitudinal transect contained insufficient data for parameterization. X.1 contained no usable data for any date, whilst X.18 and X.19 were both missing crucial data early in the growing season which prevented accurate identification of the EOW and SOS dates upon which the parameterization procedure are based. These three sites are excluded from further trend analysis, and will be considered further in the discussion section of this work. The remaining 22 sites all provided continuous time series of data suitable for parameterization. The period of available data varied between sites, from DOY 57 to DOY 273 for sites X.2 to X.8, DOY 57 to DOY 281 for sites X.9 to X.20, and DOY 49 to DOY 281 for sites X.21 to X.25. Site X.2 is the furthest west of the longitudinal sites; X.25 is the furthest east. Increasing site numbers indicate increasing longitude.

Figure 11 shows variability in P1 and P2 along the transect. P1 shows a generally decreasing trend from west to east, though two anomalously high values are present at sites X.20 and X.21, adjacent to the sites with missing spring data. P2 also has a decreasing trend between sites X.2 and X.16, after which a slight rise is present from site X.17 until the end of the transect. Spring length varies between 8 days and 24 days within the transect sites. The furthest east and west sites have spring lengths of 16 days, whilst many of the intervening sites have spring lengths of 8 days. However a small number of sites towards the middle of the transect have longer spring lengths of 16 and 24 days.

The variability in P3 is shown in Figure 12. With the exception of an anomalously positive mean winter NDVI at X.2, sites to the west of the transect exhibit negative P3 values with no significant trend. P3 values show a consistent upwards trend between X.11 and X.16. Mean winter NDVI values exceed zero from site X.14 to site X.25, though there is noticeable variability towards the east of the transect. P4 values for the longitudinal transect are plotted in Figure 13. Here X.2 again shows an anomalously high value. A linear positive trend of moderate strength is present between X.3 and X.17. A general decrease in P4 is seen between the peak at X.17 and the end of the transect at X.25, though values at the eastern end of the transect remain considerably higher than their counterparts at the western end. The along transect variability in P7, as shown in Figure 14, has no overall trend. The P7 values of the first four sites form a negative correlation along the transect, central P7 values show a weak positive correlation with site number, and eastern P7 values are strongly negatively correlated.

Table 6 shows the comparison of calculated and measured results for the date and value of maximum NDVI. Figure 15 shows longitudinal variation in the measured date of maximum NDVI and P5. Measured maximum NDVI occurs on one of three dates – DOY 201, 209 or 217.

Vegetation at eastern sites tends to reach maximum NDVI earlier than at western sites. The two sites where maximum NDVI is reached on DOY 217 fall within the western half of the transect. Of the remaining nine sites completing the western section of the transect, maximum NDVI is reached on DOY 201 at only three, compared to nine out of the eleven sites forming the eastern section of the transect. Overall, P5 follows a similar trend, with lower values further to the east, however a large amount of variability is present within this data series which does not reflect variation in measured maximum NDVI dates. Part of this variation is caused by the comparison between a discrete dataset and a continuous dataset. The residuals plotted in Figure 16 suggest that P5 is much more likely to overestimate the actual date than underestimate it throughout the transect, though the extent of this disparity varies, and there is no meaningful along-transect pattern in the errors resulting from this parameterization process. Of the four sites where P5 underestimates, the measured date of maximum NDVI is DOY 217 in two cases, and DOY 209 in the other two. Sites where the measured date of maximum NDVI falls on DOY 201 are consistently overestimated.

Both the measured maximum NDVI and P6 demonstrate higher values towards the eastern extents of the transect than the western extents, as shown in Figure 17. Both the measured maximum NDVI and P6 are approximately 0.12 higher at site X.25 than at site X.2. The nature of the upwards trend between the two sites is linear. The only major anomaly present occurs at site X.17, where the measured maximum NDVI is over 0.1 lower than that of any other site, and up to 0.2 lower than might be expected given its longitudinal position within the transect. This variation is not reflected in the P6 value calculated for the same site, causing a highly anomalous residual of -0.2234, which appears prominently in Figure 18. By comparison, the next greatest residual is +0.1375, whilst the next greatest negative residual is -0.0550. These are the only three residuals which fall outside of the ±0.05 region. Unlike the P5 residuals, the P6 residuals for the transect show only a very minor skew towards being positive, suggesting a slight underestimation of the measured maximum NDVI by P6 on average, though this is likely to be significantly affected by the negative outlier at X.17.

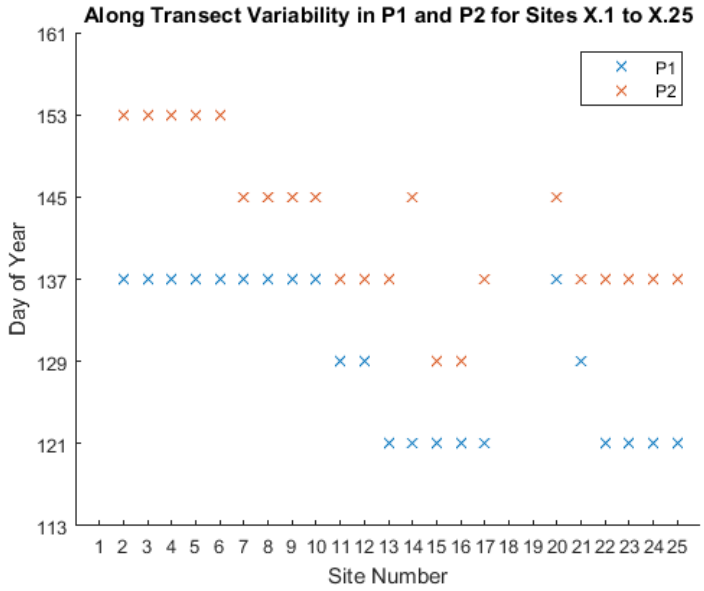


Figure 11: Graph showing along-transect variability in P1 and P2 for the longitudinal transect.

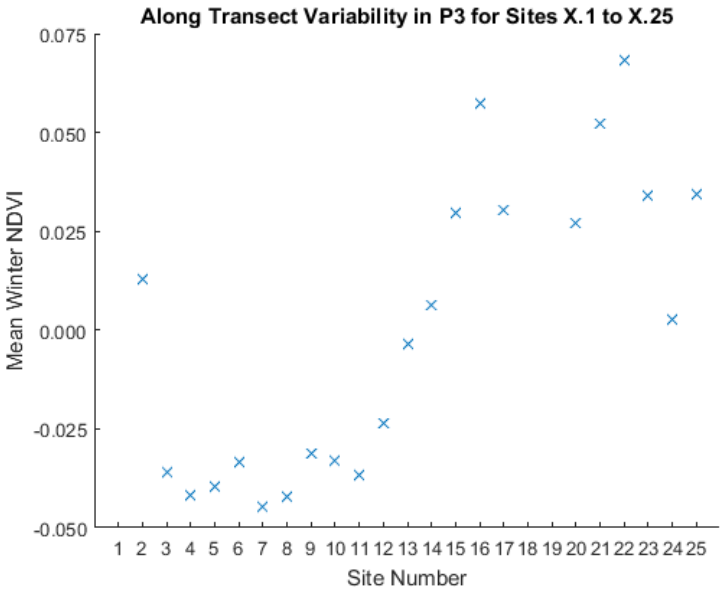


Figure 12: Graph showing along-transect variability in P3 for the longitudinal transect.

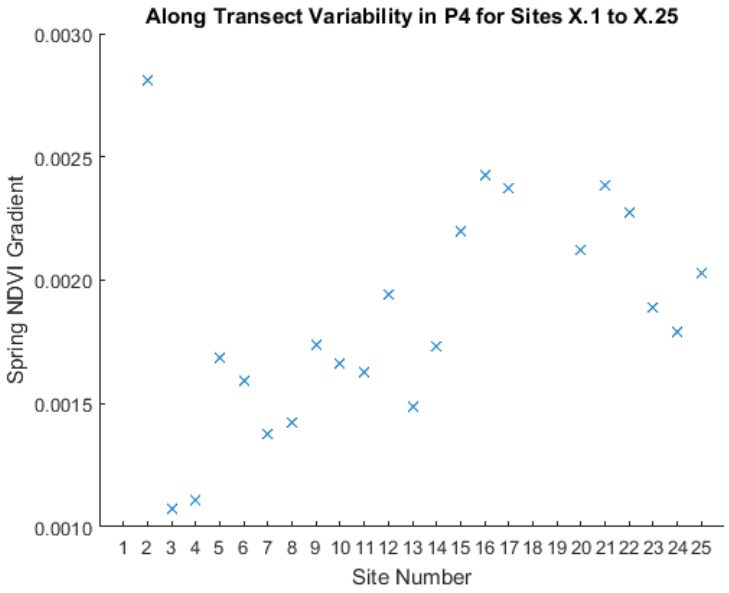


Figure 13: Graph showing along-transect variability in P4 for the longitudinal transect.

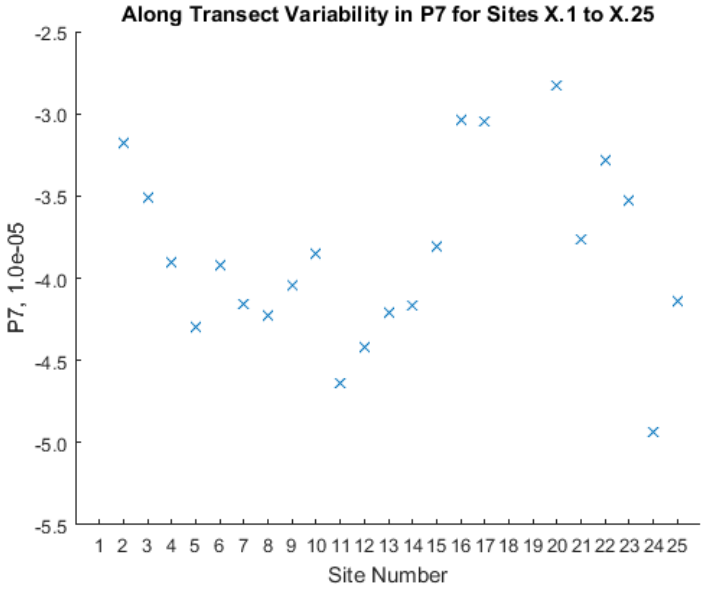


Figure 14: Graph showing along-transect variability in P7 for the longitudinal transect.

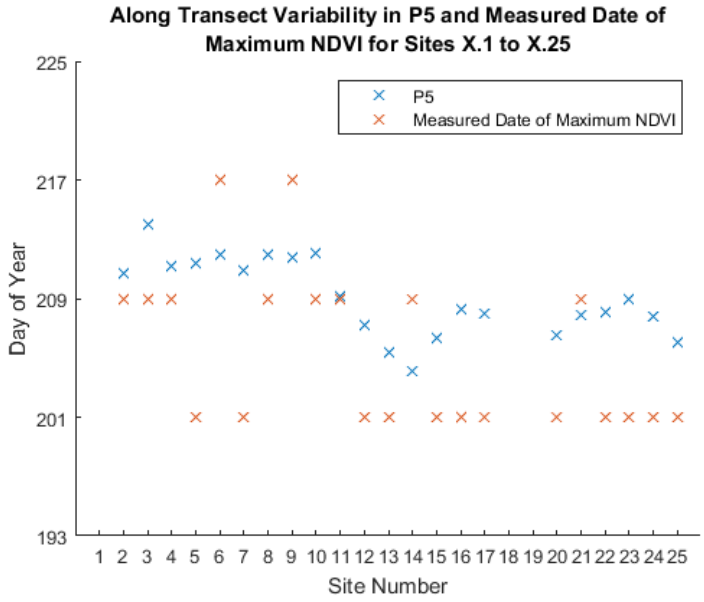


Figure 15: Graph showing along-transect variability in P5 and the measured date of maximum NDVI for the longitudinal transect.

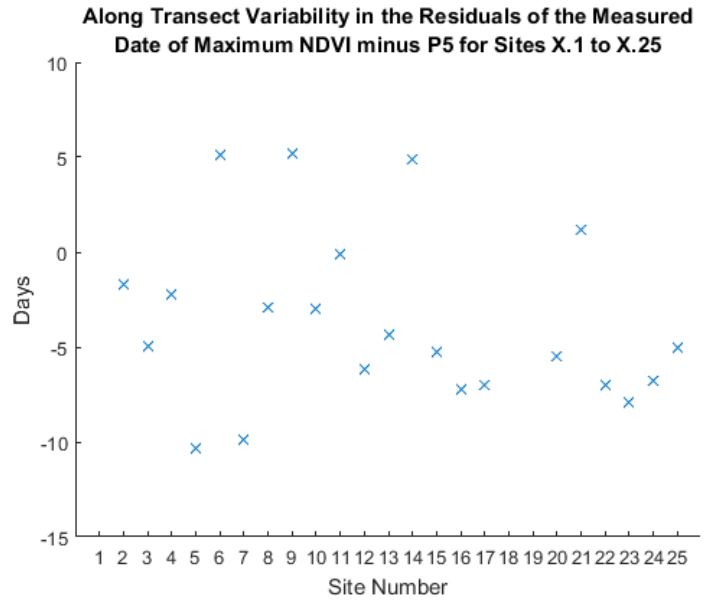


Figure 16: Graph showing along-transect variability in the residuals between P5 and the measured date of maximum NDVI for the longitudinal transect.

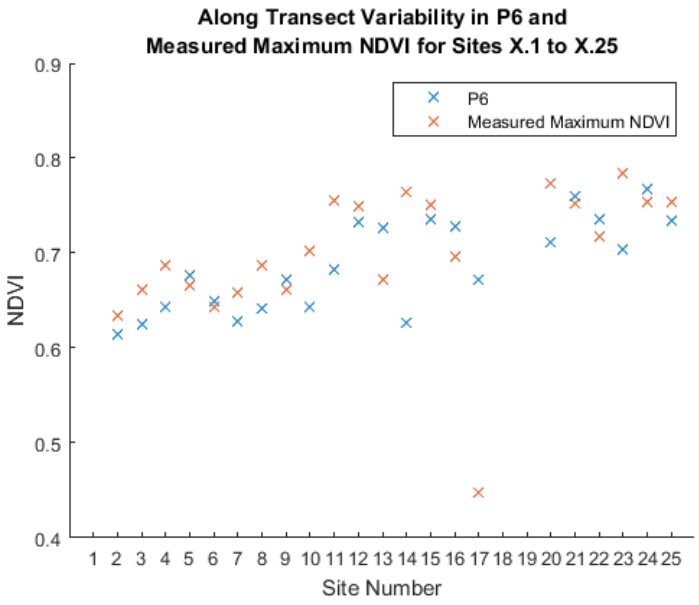


Figure 17: Graph showing along-transect variability in P6 and the measured maximum NDVI for the longitudinal transect.

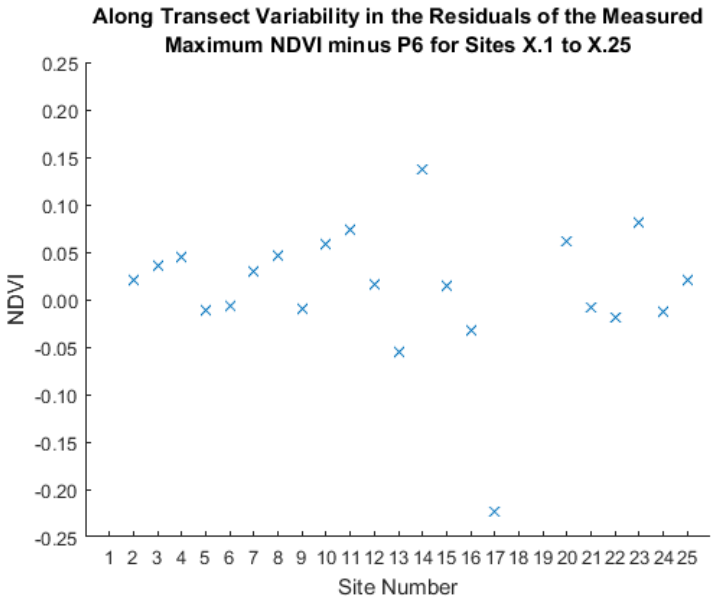


Figure 18: Graph showing along-transect variability in the residuals between P6 and the measured maximum NDVI for the longitudinal transect.

| Transect | Site | P1 | P2 | P2-P1 | P3 | P4 | P5 | P6 | P7 |
|---|---|---|---|---|---|---|---|---|---|
| **X** | **1** | | | | | | | | |
| | **2** | 137 | 153 | 16 | 0.012702 | 0.002812 | 210.71 | 0.61499 | -3.18E-05 |
| | **3** | 137 | 153 | 16 | -0.035988 | 0.001073 | 213.99 | 0.62517 | -3.51E-05 |
| | **4** | 137 | 153 | 16 | -0.041807 | 0.001108 | 211.22 | 0.64317 | -3.90E-05 |
| | **5** | 137 | 153 | 16 | -0.039682 | 0.001684 | 211.37 | 0.67723 | -4.30E-05 |
| | **6** | 137 | 153 | 16 | -0.033552 | 0.001594 | 211.91 | 0.64992 | -3.92E-05 |
| | **7** | 137 | 145 | 8 | -0.044792 | 0.001376 | 210.89 | 0.62811 | -4.16E-05 |
| | **8** | 137 | 145 | 8 | -0.042103 | 0.001422 | 211.93 | 0.64174 | -4.23E-05 |
| | **9** | 137 | 145 | 8 | -0.031169 | 0.001736 | 211.78 | 0.6717 | -4.04E-05 |
| | **10** | 137 | 145 | 8 | -0.033048 | 0.001662 | 212.03 | 0.64351 | -3.85E-05 |
| | **11** | 129 | 137 | 8 | -0.036802 | 0.001628 | 209.14 | 0.68259 | -4.64E-05 |
| | **12** | 129 | 137 | 8 | -0.023568 | 0.00194 | 207.17 | 0.73295 | -4.42E-05 |
| | **13** | 121 | 137 | 16 | -0.0036269 | 0.001488 | 205.32 | 0.72651 | -4.21E-05 |
| | **14** | 121 | 145 | 24 | 0.0064573 | 0.001732 | 204.15 | 0.62698 | -4.17E-05 |
| | **15** | 121 | 129 | 8 | 0.029727 | 0.002199 | 206.3 | 0.7358 | -3.81E-05 |
| | **16** | 121 | 129 | 8 | 0.057417 | 0.002426 | 208.26 | 0.72805 | -3.04E-05 |
| | **17** | 121 | 137 | 16 | 0.030429 | 0.002373 | 208.01 | 0.67161 | -3.05E-05 |
| | **18** | | | | | | | | |
| | **19** | | | | | | | | |
| | **20** | 137 | 145 | 8 | 0.026928 | 0.002124 | 206.5 | 0.7121 | -2.83E-05 |
| | **21** | 129 | 137 | 8 | 0.052127 | 0.002387 | 207.86 | 0.75959 | -3.76E-05 |
| | **22** | 121 | 137 | 16 | 0.068271 | 0.002273 | 208.04 | 0.73593 | -3.28E-05 |
| | **23** | 121 | 137 | 16 | 0.034078 | 0.001891 | 208.94 | 0.70405 | -3.53E-05 |
| | **24** | 121 | 137 | 16 | 0.0027364 | 0.001792 | 207.77 | 0.76705 | -4.94E-05 |
| | **25** | 121 | 137 | 16 | 0.034383 | 0.002029 | 206.02 | 0.73424 | -4.14E-05 |

Table 5: Full parameterization results for the longitudinal transect.

| Transect | Site | Date of Maximum NDVI | Date of Maximum NDVI - P5 | Maximum NDVI | Maximum NDVI - P6 |
|---|---|---|---|---|---|
| **X** | **1** | | | | |
| | **2** | 209 | -1.71 | 0.63475 | 0.01976 |
| | **3** | 209 | -4.99 | 0.66071 | 0.03554 |
| | **4** | 209 | -2.22 | 0.68739 | 0.04422 |
| | **5** | 201 | -10.37 | 0.66587 | -0.01136 |
| | **6** | 217 | 5.09 | 0.64366 | -0.00626 |
| | **7** | 201 | -9.89 | 0.6582 | 0.03009 |
| | **8** | 209 | -2.93 | 0.68766 | 0.04592 |
| | **9** | 217 | 5.22 | 0.66204 | -0.00966 |
| | **10** | 209 | -3.03 | 0.70236 | 0.05885 |
| | **11** | 209 | -0.14 | 0.75551 | 0.07292 |
| | **12** | 201 | -6.17 | 0.74924 | 0.01629 |
| | **13** | 201 | -4.32 | 0.67153 | -0.05498 |
| | **14** | 209 | 4.85 | 0.76446 | 0.13748 |
| | **15** | 201 | -5.3 | 0.75023 | 0.01443 |
| | **16** | 201 | -7.26 | 0.69583 | -0.03222 |
| | **17** | 201 | -7.01 | 0.4482 | -0.22341 |
| | **18** | | | | |
| | **19** | | | | |
| | **20** | 201 | -5.5 | 0.77327 | 0.06117 |
| | **21** | 209 | 1.14 | 0.75169 | -0.0079 |
| | **22** | 201 | -7.04 | 0.71694 | -0.01899 |
| | **23** | 201 | -7.94 | 0.78464 | 0.08059 |
| | **24** | 201 | -6.77 | 0.75399 | -0.01306 |
| | **25** | | | | |

Table 6: Comparison between measured variables and the associated parameters for the longitudinal transect. Positive values suggest an under-estimate during parameterization whilst negative values suggest an over-estimation.

### 4.6 Latitudinal Transect, Y

All 25 sites within the latitudinal transect provided sufficient data for parameterization to be undertaken; results are shown in Table 7. Site Y.1 is the further north, whilst Y.25 is the most southerly; increasing site numbers indicate decreasing latitude. The time series of data begins on DOY 57 for sites Y.1 through Y.10, Y.13, Y.22 and Y.23. Usable data is present beginning on DOY 49 at the remaining sites. The data records ends on DOY 281 at all but two sites, Y.6 and Y.7, where the record ends on DOY 273. Season length therefore varies between 216 days and 232 days, with marginally shorter growing seasons represented towards the north of the transect.

Variability in P1 and P2 along the latitudinal transect is shown in Figure 19. P1 decreases from north to south, indicating an earlier termination of winter conditions to the south. The only anomaly to this pattern occurs at site Y.2, where both P1 and P2 are 8 days later than for the surrounding sites. The length of spring is 8 days for the majority of sites within the transect. Two types of exception are identified as causing a longer spring period of 16 days: one is related to a decrease in P1, where a decrease in P2 appears to be spatially lagged, occurring at sites Y.8, Y.9 and Y.12; the other type of exception occurs between sites Y.18 and Y.23, where P1 remains steady but the associated value of P2 increases.

Figure 20 illustrates the along transect variability in P3. Whilst the first five sites indicate a slight decrease in winter NDVI with decreasing latitude, from Y.5 onwards a strong positive correlation exists between P3 and the site number. This correlation is very tight between Y.5 and Y.13, beyond which the P3 values become more scattered relative to site number. The highest mean winter NDVI of 0.0259 is associated with site Y.21. P4 shows a positive linear correlation throughout the latitudinal transect, shown in Figure 21. Slightly outlying values occur for sites Y.9 and Y.12, both of which have 16-day spring periods. Y.9 is positively outlying, whilst Y.12 is negatively outlying. With the exception of Y.19, the sites towards the south of the transect which showed longer 16-day spring periods associated with later start of summer dates all appear to have slightly elevated spring NDVI gradients in comparison to the proximate sites with 8-day spring periods. Figure 22 shows the along transect variability in P7. No trend in P7 is apparent in this data, although the spread of the data points is smaller for the sites further to the south.

Along transect variability in P5 and the measured date of maximum NDVI is shown in Figure 23, with the full numerical results shown in Table 8. The measured maximum NDVI is reached on either DOY 201 or DOY 209 at all but two sites within the transect. The anomalous sites are Y.23 and Y.24, both of which reach maximum measured NDVI on DOY 185, 16 days earlier than any other site. No clear trend is present in this series of data, and the associated P5

values show little relation to the measured values of maximum NDVI. P5 values generally trend slightly downwards with decreasing latitude, however sites Y.21 to Y.25 exhibit a slight increase in P5, indicating that maximum NDVI is reached slightly later – this directly contrasts the measured values, which reach a minimum within this range. The majority of P5 values throughout the transect fall between DOY 207 and DOY 214, and therefore tend to overestimate the measured values, as shown in Figure 24. This overestimation reaches a maximum of approximately 24 days at sites Y.23 and Y.24. A small number of sites between Y.16 and Y.21 produce P5 values which underestimate the measured value – this error is usually between 1.5 and 2 days, and is therefore relatively small in comparison to the systematic overestimation of between 5 and 10 days occurring at many of the other sites within the transect.

P6 values for the latitudinal transect show very close agreement to the measured maximum NDVI values, shown in Figure 25. Both data series have minima at Y.2 and maxima at Y.21. The data show a general increase in maximum NDVI with decreasing latitude. A set of three outlying values appear for sites Y.9, Y.10 and Y.11, where the maximum NDVI reached is over 0.5 below the surrounding sites. The residuals shown in Figure 26 demonstrate the closeness of the predicted P6 values to the measured maximum NDVI values. For all sites except Y.2, P6 very slightly underestimates the measured value by between 0.005 and 0.030. The P6 for Y.2 overestimates the measured maximum NDVI by only 0.003. In order to illustrate the small amplitude of the errors between measured maximum NDVI and P6 for the latitudinal transect, Figure 27 shows the residuals for this transect plotted against the vertical axis used for the same variable for the longitudinal transect.

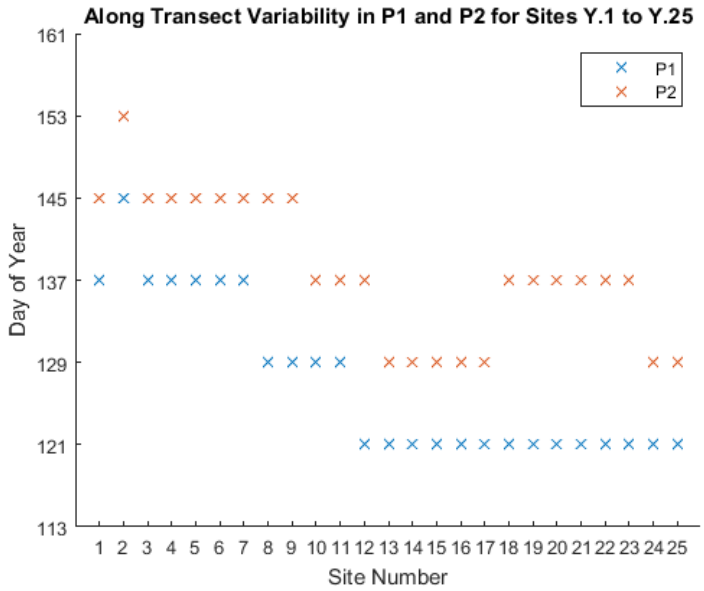


Figure 19: Graph showing along-transect variability in P1 and P2 for the latitudinal transect.

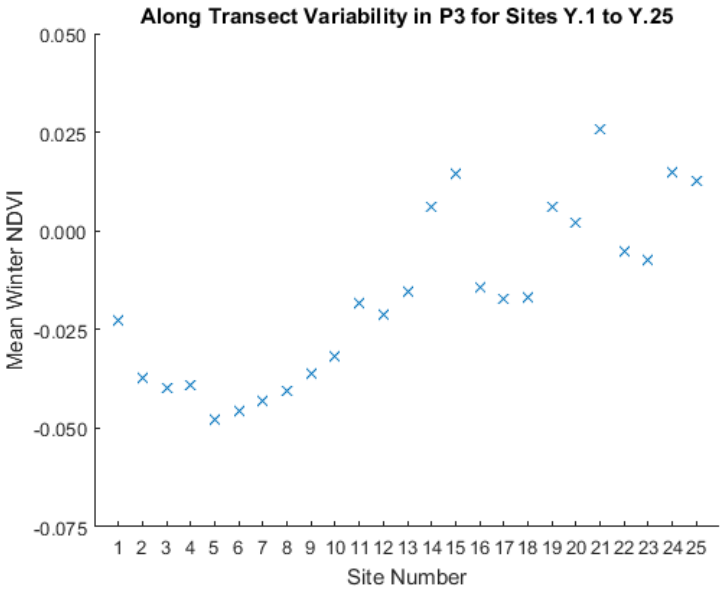


Figure 20: Graph showing along-transect variability in P3 for the latitudinal transect.

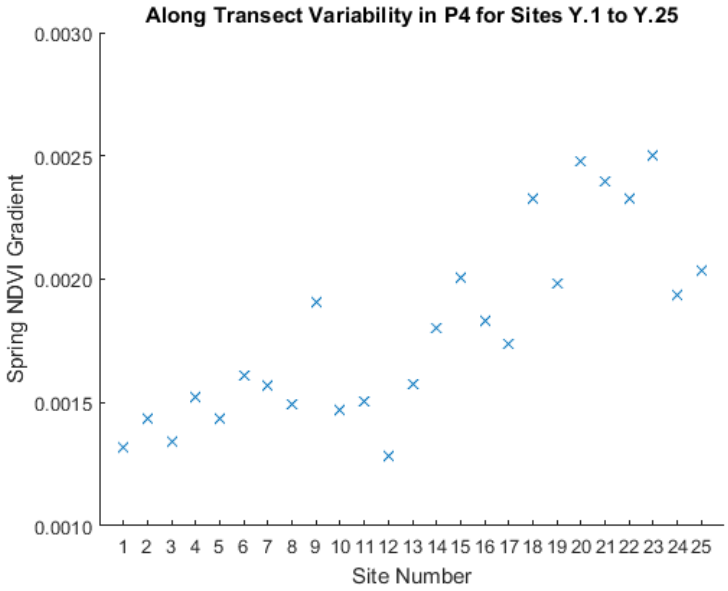


Figure 21: Graph showing along transect variability in P4 for the latitudinal transect.

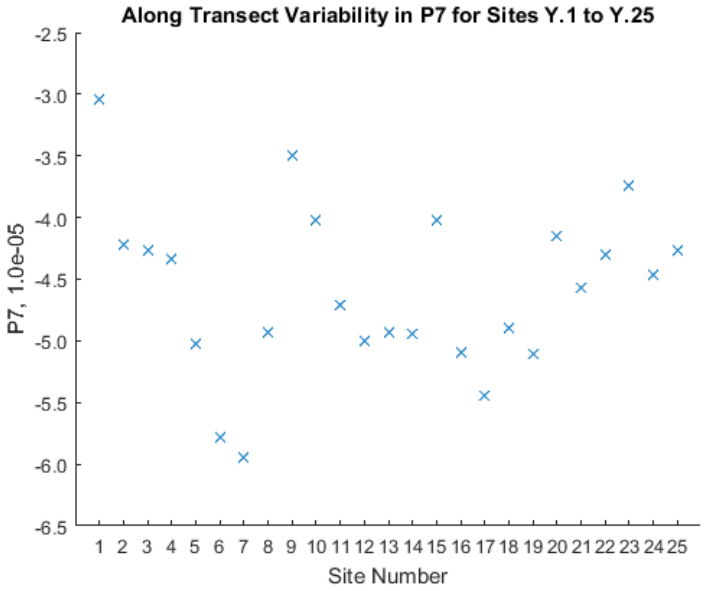


Figure 22: Graph showing along-transect variability in P7 for the latitudinal transect.

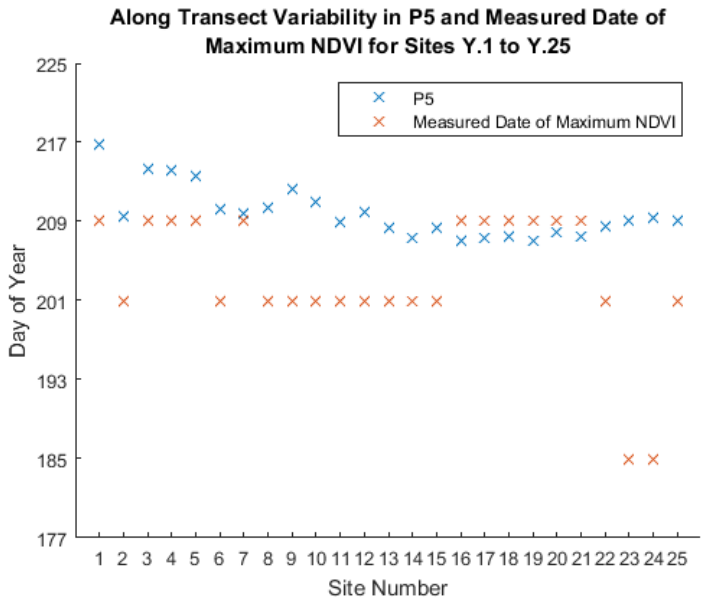


Figure 23: Graph showing along-transect variability in P5 and the measured date of maximum NDVI for the latitudinal transect.

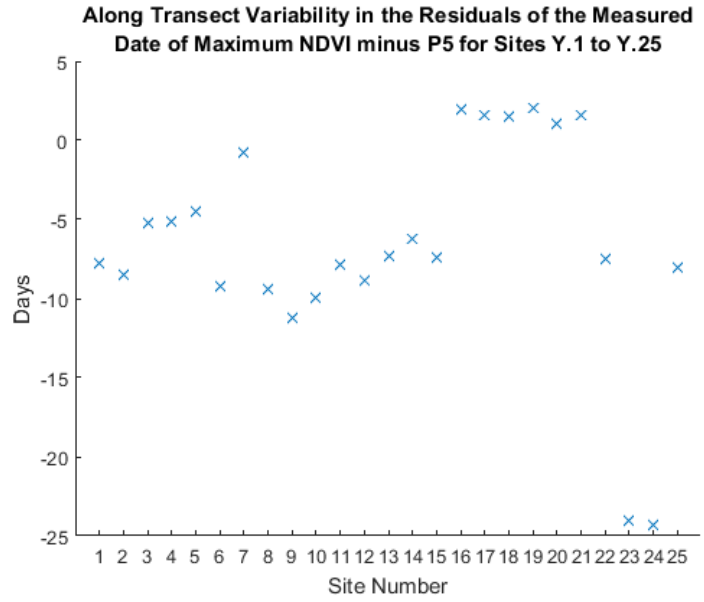


Figure 24: Graph showing along-transect variability in the residuals between P5 and the measured date of maximum NDVI for the latitudinal transect.

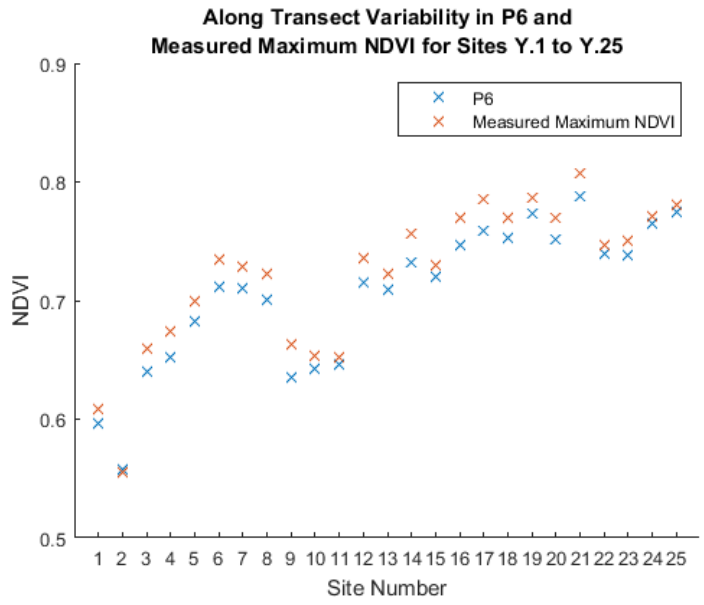


Figure 25: Graph showing along-transect variability in P6 and the measured maximum NDVI for the latitudinal transect.

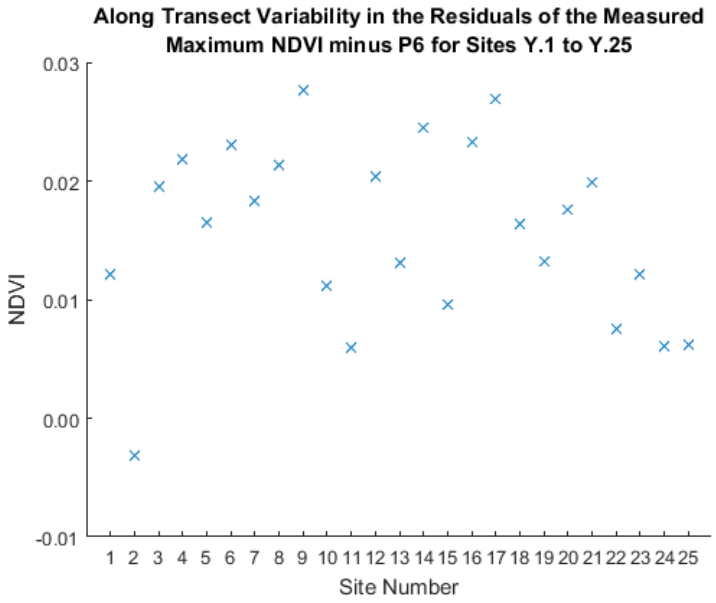


Figure 26: Graph showing along-transect variability in the residuals between P6 and the measured maximum NDVI for the latitudinal transect.

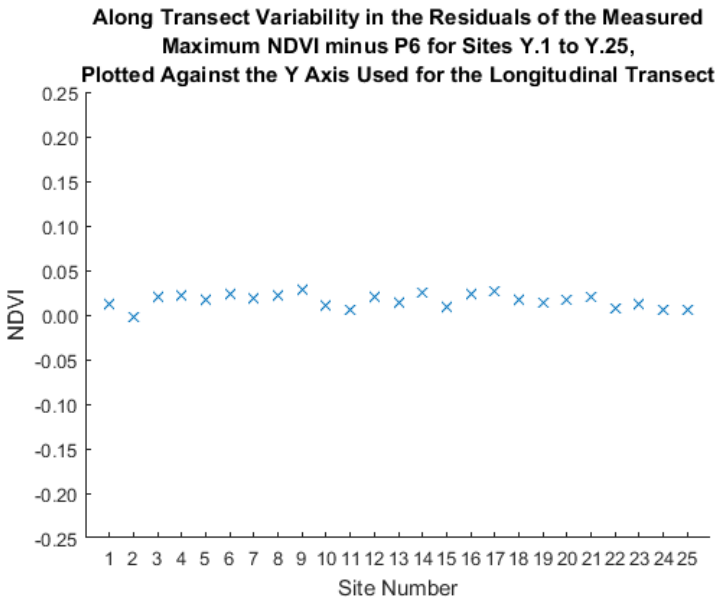


Figure 27: Graph showing along-transect variability in the residuals between P6 and the measured maximum NDVI for the latitudinal transect, plotted against the Y-axis used for the longitudinal transect, for comparative purposes.

| Transect | Site | P1 | P2 | P2-P1 | P3 | P4 | P5 | P6 | P7 |
|---|---|---|---|---|---|---|---|---|---|
| **Y** | **1** | 137 | 145 | 8 | -0.022746 | 0.001317 | 216.76 | 0.59678 | -3.04E-05 |
| | **2** | 145 | 153 | 8 | -0.037339 | 0.001437 | 209.51 | 0.55776 | -4.22E-05 |
| | **3** | 137 | 145 | 8 | -0.039859 | 0.001343 | 214.26 | 0.6396 | -4.27E-05 |
| | **4** | 137 | 145 | 8 | -0.03899 | 0.001521 | 214.12 | 0.65233 | -4.34E-05 |
| | **5** | 137 | 145 | 8 | -0.047916 | 0.001435 | 213.53 | 0.68287 | -5.03E-05 |
| | **6** | 137 | 145 | 8 | -0.045644 | 0.001608 | 210.26 | 0.71182 | -5.78E-05 |
| | **7** | 137 | 145 | 8 | -0.043135 | 0.00157 | 209.81 | 0.7106 | -5.95E-05 |
| | **8** | 129 | 145 | 16 | -0.040503 | 0.00149 | 210.39 | 0.70083 | -4.93E-05 |
| | **9** | 129 | 145 | 16 | -0.03623 | 0.001908 | 212.22 | 0.63537 | -3.50E-05 |
| | **10** | 129 | 137 | 8 | -0.031716 | 0.001471 | 210.92 | 0.64218 | -4.02E-05 |
| | **11** | 129 | 137 | 8 | -0.018295 | 0.001503 | 208.9 | 0.6459 | -4.71E-05 |
| | **12** | 121 | 137 | 16 | -0.021209 | 0.00128 | 209.9 | 0.71554 | -5.00E-05 |
| | **13** | 121 | 129 | 8 | -0.015354 | 0.001572 | 208.33 | 0.70895 | -4.93E-05 |
| | **14** | 121 | 129 | 8 | 0.0061819 | 0.001799 | 207.27 | 0.732 | -4.94E-05 |
| | **15** | 121 | 129 | 8 | 0.014495 | 0.002008 | 208.37 | 0.71989 | -4.02E-05 |
| | **16** | 121 | 129 | 8 | -0.014343 | 0.001829 | 207.04 | 0.74645 | -5.09E-05 |
| | **17** | 121 | 129 | 8 | -0.017254 | 0.001739 | 207.39 | 0.75889 | -5.44E-05 |
| | **18** | 121 | 137 | 16 | -0.017006 | 0.002325 | 207.49 | 0.75317 | -4.90E-05 |
| | **19** | 121 | 137 | 16 | 0.0059293 | 0.001984 | 206.98 | 0.77307 | -5.11E-05 |
| | **20** | 121 | 137 | 16 | 0.0021615 | 0.002479 | 207.97 | 0.75182 | -4.15E-05 |
| | **21** | 121 | 137 | 16 | 0.02592 | 0.002394 | 207.42 | 0.7873 | -4.57E-05 |
| | **22** | 121 | 137 | 16 | -0.0050727 | 0.002327 | 208.47 | 0.7394 | -4.30E-05 |
| | **23** | 121 | 137 | 16 | -0.007286 | 0.002504 | 209.08 | 0.73766 | -3.74E-05 |
| | **24** | 121 | 129 | 8 | 0.014837 | 0.001938 | 209.3 | 0.76522 | -4.46E-05 |
| | **25** | 121 | 129 | 8 | 0.012653 | 0.002033 | 209.08 | 0.77425 | -4.27E-05 |

Table 7: Full parameterization results for the latitudinal transect.

| Transect | Site | Date of Maximum NDVI | Date of Maximum NDVI - P5 | Maximum NDVI | Maximum NDVI - P6 |
|---|---|---|---|---|---|
| **Y** | **1** | 209 | -7.76 | 0.6089 | 0.01212 |
| | **2** | 201 | -8.51 | 0.55459 | -0.00317 |
| | **3** | 209 | -5.26 | 0.65915 | 0.01955 |
| | **4** | 209 | -5.12 | 0.67419 | 0.02186 |
| | **5** | 209 | -4.53 | 0.6993 | 0.01643 |
| | **6** | 201 | -9.26 | 0.7348 | 0.02298 |
| | **7** | 209 | -0.81 | 0.7289 | 0.0183 |
| | **8** | 201 | -9.39 | 0.72222 | 0.02139 |
| | **9** | 201 | -11.22 | 0.66305 | 0.02768 |
| | **10** | 201 | -9.92 | 0.65339 | 0.01121 |
| | **11** | 201 | -7.9 | 0.65189 | 0.00599 |
| | **12** | 201 | -8.9 | 0.73587 | 0.02033 |
| | **13** | 201 | -7.33 | 0.72205 | 0.0131 |
| | **14** | 201 | -6.27 | 0.75645 | 0.02445 |
| | **15** | 201 | -7.37 | 0.72941 | 0.00952 |
| | **16** | 209 | 1.96 | 0.76974 | 0.02329 |
| | **17** | 209 | 1.61 | 0.78581 | 0.02692 |
| | **18** | 209 | 1.51 | 0.7695 | 0.01633 |
| | **19** | 209 | 2.02 | 0.78626 | 0.01319 |
| | **20** | 209 | 1.03 | 0.7694 | 0.01758 |
| | **21** | 209 | 1.58 | 0.80722 | 0.01992 |
| | **22** | 201 | -7.47 | 0.7469 | 0.0075 |
| | **23** | 185 | -24.08 | 0.74979 | 0.01213 |
| | **24** | 185 | -24.3 | 0.77123 | 0.00601 |
| | **25** | 201 | -8.08 | 0.7804 | 0.00615 |

Table 8: Comparison between measured variables and the associated parameters for the latitudinal transect. Positive values suggest an under-estimate during parameterization whilst negative values suggest an over-estimation.

## 4.7 Biomization of the Longitudinal and Latitudinal Transects

The results of the investigation into the differentiation of tundra and taiga vegetation based on phenological parameters have been applied to the X and Y transects in order to further assess the methodology. Table 9 shows the parameter ranges established based on the data extracted from transects T1, T2, F1 and F2; P7 is excluded due to the large amount of overlap found between tundra and taiga sites for this parameter. These boundaries are applied to the data from transects X and Y in Table 10 and Table 11 respectively, using conditional formatting in order to visually illustrate spatial vegetation gradients.

Table 10 shows that the majority of western sites within the longitudinal transect produce parameters which are closely related to those associated with the tundra transects. Site X.2 shows outlying values of P3 and P4, with both falling within the range indicating taiga vegetation. Sites X.3 through X.11 show non-ambiguous parameters in line with values expected of tundra vegetation. Sites further to the east have an increased affinity with the results of the taiga analysis, however site X.16 is the only site where all non-ambiguous parameters indicate taiga vegetation; all other sites show a mixture of results aligned with both tundra and taiga parameter ranges.

Table 11 illustrates a significant north-south pattern in the parameterization results of the latitudinal transect. Sites Y.1 to Y.12 are characterised only by parameters that either indicate tundra vegetation or fall into the ambiguous ranges. Sites Y.13 to Y.25 produce parameters which are, for the most part, either aligned with the results of the taiga transects or ambiguous. The major exception is a stretch of sites from Y.18 through Y.23 which have start of summer dates falling within the tundra range, though no other parameters indicate tundra vegetation. Sites Y.1 though Y.13 all have P6 values suggesting tundra; sites Y.16 through Y.25 all have P6 values suggesting taiga. It is this parameter which appears to most clearly be correlated with latitude based on this transect.

| | P1 | P2 | P3 | P4 | P5 | P6 |
|---|---|---|---|---|---|---|
| **Out of range – beyond taiga limit** | <121 | <129 | >0.0860 | >0.002643 | <204.39 | >0.78769 |
| **Taiga** | | 129 | 0.0022 to 0.0860 | 0.002254 to 0.002643 | 204.39 to 207.85 | 0.72650 to 0.78769 |
| **Ambiguous** | 121 | | -0.0360 to 0.0022 | 0.001926 to 0.002254 | 207.85 to 210.32 | 0.72266 to 0.72650 |
| **Tundra** | 129 to 137 | 137 to 153 | -0.0459 To -0.036 | 0.001113 to 0.001926 | 210.32 to 215.49 | 0.6557 to 0.72266 |
| **Out of range – beyond tundra limit** | >137 | >153 | <-0.0459 | <0.001113 | >215.49 | <0.65570 |

Table 9: Biome parameter boundaries. Ambiguous results either fall into areas of overlap between the tundra and taiga transects (P1, 4) or fall between the measured ranges for the two transects (P2, 5, 6).

| Transect | Site | P1 | P2 | P3 | P4 | P5 | P6 |
|---|---|---|---|---|---|---|---|
| **X** | **1** | | | | | | |
| | **2** | 137 | 153 | 0.012702 | 0.002812 | 210.71 | 0.61499 |
| | **3** | 137 | 153 | -0.03599 | 0.001073 | 213.99 | 0.62517 |
| | **4** | 137 | 153 | -0.04181 | 0.001108 | 211.22 | 0.64317 |
| | **5** | 137 | 153 | -0.03968 | 0.001684 | 211.37 | 0.67723 |
| | **6** | 137 | 153 | -0.03355 | 0.001594 | 211.91 | 0.64992 |
| | **7** | 137 | 145 | -0.04479 | 0.001376 | 210.89 | 0.62811 |
| | **8** | 137 | 145 | -0.0421 | 0.001422 | 211.93 | 0.64174 |
| | **9** | 137 | 145 | -0.03117 | 0.001736 | 211.78 | 0.6717 |
| | **10** | 137 | 145 | -0.03305 | 0.001662 | 212.03 | 0.64351 |
| | **11** | 129 | 137 | -0.0368 | 0.001628 | 209.14 | 0.68259 |
| | **12** | 129 | 137 | -0.02357 | 0.00194 | 207.17 | 0.73295 |
| | **13** | 121 | 137 | -0.00363 | 0.001488 | 205.32 | 0.72651 |
| | **14** | 121 | 145 | 0.006457 | 0.001732 | 204.15 | 0.62698 |
| | **15** | 121 | 129 | 0.029727 | 0.002199 | 206.3 | 0.7358 |
| | **16** | 121 | 129 | 0.057417 | 0.002426 | 208.26 | 0.72805 |
| | **17** | 121 | 137 | 0.030429 | 0.002373 | 208.01 | 0.67161 |
| | **18** | | | | | | |
| | **19** | | | | | | |
| | **20** | 137 | 145 | 0.026928 | 0.002124 | 206.5 | 0.7121 |
| | **21** | 129 | 137 | 0.052127 | 0.002387 | 207.86 | 0.75959 |
| | **22** | 121 | 137 | 0.068271 | 0.002273 | 208.04 | 0.73593 |
| | **23** | 121 | 137 | 0.034078 | 0.001891 | 208.94 | 0.70405 |
| | **24** | 121 | 137 | 0.002736 | 0.001792 | 207.77 | 0.76705 |
| | **25** | 121 | 137 | 0.034383 | 0.002029 | 206.02 | 0.73424 |

Table 10: Biomization results for the longitudinal transect. Colour legend shown in Table 9.

| Transect | Site | P1 | P2 | P3 | P4 | P5 | P6 |
|---|---|---|---|---|---|---|---|
| Y | 1 | 137 | 145 | -0.02275 | 0.001317 | 216.76 | 0.59678 |
| | 2 | 145 | 153 | -0.03734 | 0.001437 | 209.51 | 0.55776 |
| | 3 | 137 | 145 | -0.03986 | 0.001343 | 214.26 | 0.6396 |
| | 4 | 137 | 145 | -0.03899 | 0.001521 | 214.12 | 0.65233 |
| | 5 | 137 | 145 | -0.04792 | 0.001435 | 213.53 | 0.68287 |
| | 6 | 137 | 145 | -0.04564 | 0.001608 | 210.26 | 0.71182 |
| | 7 | 137 | 145 | -0.04314 | 0.00157 | 209.81 | 0.7106 |
| | 8 | 129 | 145 | -0.0405 | 0.00149 | 210.39 | 0.70083 |
| | 9 | 129 | 145 | -0.03623 | 0.001908 | 212.22 | 0.63537 |
| | 10 | 129 | 137 | -0.03172 | 0.001471 | 210.92 | 0.64218 |
| | 11 | 129 | 137 | -0.0183 | 0.001503 | 208.9 | 0.6459 |
| | 12 | 121 | 137 | -0.02121 | 0.00128 | 209.9 | 0.71554 |
| | 13 | 121 | 129 | -0.01535 | 0.001572 | 208.33 | 0.70895 |
| | 14 | 121 | 129 | 0.006182 | 0.001799 | 207.27 | 0.732 |
| | 15 | 121 | 129 | 0.014495 | 0.002008 | 208.37 | 0.71989 |
| | 16 | 121 | 129 | -0.01434 | 0.001829 | 207.04 | 0.74645 |
| | 17 | 121 | 129 | -0.01725 | 0.001739 | 207.39 | 0.75889 |
| | 18 | 121 | 137 | -0.01701 | 0.002325 | 207.49 | 0.75317 |
| | 19 | 121 | 137 | 0.005929 | 0.001984 | 206.98 | 0.77307 |
| | 20 | 121 | 137 | 0.002162 | 0.002479 | 207.97 | 0.75182 |
| | 21 | 121 | 137 | 0.02592 | 0.002394 | 207.42 | 0.7873 |
| | 22 | 121 | 137 | -0.00507 | 0.002327 | 208.47 | 0.7394 |
| | 23 | 121 | 137 | -0.00729 | 0.002504 | 209.08 | 0.73766 |
| | 24 | 121 | 129 | 0.014837 | 0.001938 | 209.3 | 0.76522 |
| | 25 | 121 | 129 | 0.012653 | 0.002033 | 209.08 | 0.77425 |

Table 11: Biomization results for the latitudinal transect. Colour legend shown in Table 9.

# 5 – Discussion

## 5.1 Differentiation of Tundra and Taiga Vegetation Using Calculated Parameters

The results gained from the tundra and taiga sites show strong agreement within individual transects, and good agreement between transects of the same vegetation type. Both tundra and taiga sites show similar annual trends: low winter NDVI values early in the year; a sharp rise during spring; a continued increase at a subdued rate to a summer peak; a small but noticeable decrease later in the year associated with the end of summer; and a relatively flat autumnal signal until the end of the data record. However the timing and amplitude of these effects as represented by the parameterization results varies significantly between tundra and taiga sites, whilst remaining fairly stable within each transect, as well as between transects representing the same biome. These results suggest there may be some ability to differentiate between vegetation of the two biomes using the parameters calculated from annual phenological profiles.

P3 is consistently above zero for taiga transects, but consistently below zero for tundra transects. P1 is earlier for all taiga sites than for all but one of the tundra sites, and P2 is earlier for all taiga sites than for all tundra sites. The calculated length of spring has some overlap between biomes, but is 5.6 days longer on average for tundra sites than the consistent 8-day spring of taiga sites. The mean P4 value for tundra sites is 0.000672 lower than that of taiga sites, with only one tundra site showing a rate of spring increase higher than any of the taiga sites. Whilst all of these variables show some potential for discerning between biomes, the most distinct difference is present in P2, suggesting that the start of summer date is the most suitable early season parameter for discriminating tundra from taiga.

On average, P5 values occur almost a week earlier in taiga sites than tundra sites, and there is no overlap between the earliest tundra P5 value and the latest taiga P5 value. This contrasts the fact that the measured date of maximum NDVI is DOY 201 for all ten tundra sites, and eight of the taiga sites – a contrast that indicates that the parameters may offer better differentiation between vegetation types than the measured value. The associated P6 values average 0.06741 higher at taiga sites than at tundra sites, and the highest tundra value is lower than the lowest taiga value, therefore there is no overlap between the P6 values of the two biomes. A similar pattern is reflected in the measured maximum NDVI values, which average 0.06181 higher across all taiga sites than all tundra sites. However the tundra site with the highest measured maximum NDVI slightly exceeds that of two of the taiga sites, therefore these datasets are not discrete of one another. The level of difference indicates that either P6 or the measured maximum NDVI could be used to discriminate between the two types of vegetation, though once again the parameter shows a more pronounced distinction than the measured

value. This suggests that the parameterization procedure adds value to the data for the purpose of facilitating differentiation between vegetation zones.

Of all of the parameterized variables, P7 shows the least differentiation between the sites of the chosen tundra and taiga transects, with overlapping values across all four transects. Although on average the curvature of the summer trendlines for tundra sites is slightly greater than those of the taiga sites, the overlap in calculated values does not suggest that this parameter would be suitable for differentiating between the two biomes. The timing of the autumn signal cannot be further included here as it has only been qualitatively assessed, and was not parameterized quantitatively; this methodological limitation will be further discussed later, as autumn data could potentially provide more insight into phenological differentiation of tundra and taiga vegetation. However this is not considered to be a critical failing, as previous studies have found spring phenological signals to be more responsive to vegetation change than autumn signals (Sparks and Menzel, 2002).

Overall the parameterization of phenological profiles based on NDVI data shows good success in differentiating between the tundra and taiga sites. The boundary values for each parameter representing each of the two biomes is shown in Table 12. P2, P3, P5 and P6 all have value ranges which are discrete to each biome. It is therefore possible that these parameters – or some combination thereof – could be used to determine the biome designation of an unknown site. Furthermore, values lying at the boundaries of, or between, the ranges found here could indicate transitional sites constituent of the TTE. One limiting consideration is whether or not these differences are reflective of on-the-ground differences in biome, or whether they are simply a product of latitude, as both tundra sites are at higher latitudes than both taiga sites. This issue will be addressed further following discussion of the results from the latitudinal transect.

| **Biome** | | **P1** | **P2** | **P3** | **P4** | **P5** | **P6** | **P7** |
|---|---|---|---|---|---|---|---|---|
| **Tundra** | Min | 121 | 137 | -0.0459 | 0.001113 | 210.32 | 0.65570 | -4.97E-05 |
| | Max | 137 | 153 | -0.0360 | 0.002253 | 215.49 | 0.72266 | -3.63E-05 |
| **Taiga** | Min | 121 | 129 | 0.0022 | 0.001927 | 204.39 | 0.72650 | -4.72E-05 |
| | Max | 121 | 129 | 0.0860 | 0.002643 | 207.85 | 0.78769 | -3.19E-05 |

Table 12: Parameter boundary values across all sites representing each biome. Parameters with green shading show no overlap between the two biomes; those with orange shading have limited overlap, but remain quite distinct; and those with red shading have large amounts of overlap, and are not suitable for differentiating between vegetation types.

## 5.2 Altitudinal and Technogenic Vegetation Gradients

Results from the Khibiny and Monchegorsk transects indicate that both altitude and anthropogenic influence can create regions lacking sufficient good quality MODIS pixels for analysis. This lack of good quality data is particularly pronounced at altitude, with three of the Khibiny sites providing insufficient data for parameterization of the phenological profile to be undertaken, in comparison to one of the Monchegorsk sites. The poor density of good quality pixels over the Khibiny transect is thought to be due to a combination of perennial snow cover – with glaciers, icefields and snowfields present in areas of the massif – and persistent cloud cover related to orographic production (EU Interact, 2017; Demin and Zyuzin, 2006). The lack of data from the Monchegorsk site is directly related to the technogenic barren, which is in part a result of high levels of atmospheric pollution caused by industrial emissions, which obscure multispectral imaging of the surface of the earth (Shipigina and Rees, 2012; Rees and Williams, 1997).

Based on the limited raw data available from sites M.1 and K.3 to K.5, it appears that qualitative differentiation between regions lacking sufficient data for parameterization due to altitudinal and technogenic influences may be possible. Sites K.3 to K.5 consistently provide winter data between DOY 81 and DOY 129, but lack good quality NDVI data during the spring period at site K.3, and throughout the spring and summer seasons at sites K.4 and K.5. In contrast, site M.1 lacks winter data, containing only a very limited number of data points during some summer months. Whilst the difference in these patterns is distinct, no strict conclusions can be drawn due to the very limited number of sites for which such data is available – further investigation of regions at altitude and in regions under strong anthropogenic influence would be required to substantiate the significance of these observations. One key aspect in determining whether or not these differences are significant is identifying the forcing factors which cause these persistent data voids between years, for example if the lack of data for the sites at altitude could be attributed to orographic production of spring cloud cover.

The identification of trends within the Khibiny transect is not undertaken due to a combination of the facts that parameters are only available from two sites, and that neither of these sites has results analogous to any gathered for the known tundra and taiga vegetation transects. Site K.1 has both a very high P3 value and a very high P5 value, whilst site K.2 has a very low P3 value and a very low P5 value – these relationships between variables contradict the overall negative correlation of -0.302 between P3 and P5 across all sites. The Khibiny summer trend lines also show the two lowest curvatures of all sites studied, at -1.65E-05 and -2.01E-05. Whilst it is possible that the influence of altitude causes these novel effects, there is insufficient data to test this, therefore no reliable conclusion can be drawn. The only clear feature worth

noting for future reference is the dramatic decrease in P6 which occurs at site K.2, where P6 falls below that of many tundra sites.

In order to better quantify the effect of altitude on phenology, it is likely that smaller sites would need to be designated. Whilst altitudinal vegetation gradients are often seen as analogues for broader latitudinal vegetation gradients, mimicking the associated biome shifts, these changes occur over a much shorter horizontal distance when forced by altitude than when forced by latitude (Kharuk *et al*, 2007; Beck *et al*, 2007). It is therefore probable that the 2.5 $km^2$ site size used in this study obscures significant smaller scale vegetation changes. This could be particularly important in areas of high relief due to the considerable impact of aspect on vegetation growth. Whilst work using smaller study sites could be undertaken using a decreased number of MODIS pixels, the use of a higher spatial resolution remote sensing data set such as Landsat could prove more successful for investigating such localised vegetation gradients. This is an area for future research, as applying the methodology developed herein to Landsat data is beyond the scope of the present investigation.

The clearest trend arising from the Monchegorsk data is that sites closer to the technogenic barren to the west of the transect have lower maximum NDVI values than those further to the east. Sites M.2 and M.3 have the two lowest calculated P6 values across all sites studied, at 0.44751 and 0.51373 respectively. This suggests that the anthropogenic influence of heavy industrialization either causes a shift in species composition, or suppresses vegetation growth entirely. An alternative explanation is that sites to the west of the transect have been influenced by a fire regime driven by the death of boreal forest vegetation due to elevated toxicity levels, and that the loss of vegetation due to burning is therefore contributing to the suppression of maximum NDVI values – this is an environmental factor that has been identified in the region by Shipigina and Rees (2012). The fact that all P6 values calculated for the Monchegorsk transect are below all of the P6 values calculated for the tundra and taiga sites indicates the significance of the anthropogenic impact on the area, regardless of which of the posited mechanisms is driving the change.

No other parameter emerges from the Monchegorsk data as such a definitive indicator of the technogenic gradient under investigation. However qualitative analysis of Figure 10 suggests that the anthropogenic influence associated with the technogenic barren causes an increase in the spread of the data. The graphs for sites M.4 and M.5 show very close agreement between the measured median NDVI values and the fitted summer trend quadratic, whereas those for sites M.2 and M.3 have a more noticeable spread of data values around the trendline. Furthermore, increasing proximity to the technogenic barren in the west is associated with gradually increasing upwards trends in winter NDVI – although P3 is higher for M.4 than M.3,

the latter appears to have a more pronounced slope throughout the same period. This winter NDVI trend does not appear in any of the tundra or taiga sites. It is therefore considered to be a product of the anthropogenic influence, and could provide some utility for confirming this influence as a factor at other sites. Further research into other sites known to be in regions under the influence of technogenic pollution would be necessary to confirm this hypothesis. The use of smaller study sites may also be useful in this context, though the need does not appear to be as pronounced here as it is for the altitudinal gradient.

In summary, the limited extent of the Khibiny and Monchegorsk transects restricts their usefulness in characterising the effects of altitudinal and anthropogenic effects on vegetation gradients in the TTE. This limitation is more pronounced for Khibiny, likely associated with the relatively large horizontal size of individual sites relative to the scale on which altitudinal vegetation gradients occur. It is therefore not possible to draw any reliable conclusions from the available results. For the Monchegorsk transect, P6 is identified as the primary indicator of the technogenic gradient, showing a negative correlation to proximity to the barren. Qualitative assessment of the raw data also provides some insight into unusual winter NDVI trends in proximity to the technogenic barren. Results show that both anthropogenic and altitudinal effects have the potential to cause data voids which prohibit parameterization of phenological profiles, due to a lack of annual data.

### 5.3 Biomization of Regional Vegetation Transects

The longitudinal and latitudinal transects are set up in order to (i) allow examination of vegetation gradients on a regional scale, and (ii) investigate the extent to which variation in NDVI is a function of latitude, by (iii) providing test locations for attempted biomization based on the parameterization results of the phenological profiles for the tundra and taiga transects.

The results gathered from applying the tundra and taiga parameter ranges to the longitudinal and latitudinal transect results presented herein suggest that the method has some success in spatial differentiation of vegetation. Results show a fairly clear break between tundra and taiga sites for the latitudinal transect – a result that is not unexpected based on the significance of latitude controls on temperature and insolation. The fact that P6 is both the parameter with the most defined north-south divide, and produces much smaller residuals compared to the measured value for the latitudinal transect than the longitudinal transect, could indicate that variation in this parameter is strongly driven by latitude.

A small number of sites representing up to 50 km of on-the-ground distance are characterised by a combination of tundra and taiga parameters, which is potentially indicative of a region of TTE. Although latitude is clearly a major controlling factor on parameterization,

the fact that non-linear results exist for the latitudinal transect indicate the concurrent importance of other variables. For example, sites Y.9 to Y.11 have lower P6 values than the immediately surrounding sites, producing values closer to those occurring at sites 40 km to the north. This could be due to a number of factors, but a small increase in altitude is deemed most likely based on Figure 2 and results gathered from the Khibiny transect. It is not possible based on the results from the latitudinal transect to determine any influence of continentality on vegetation, perhaps due to the small size of the Kola Peninsula.

The significant amount of variability within the longitudinal transect further demonstrates that a number of factors must have a significant impact on vegetation behaviours based on the parameters used in this study. Site X.1 is not at altitude, therefore the lack of useable results from this site is thought to be the result of anthropogenic impacts – the high values of P3 and P4 at site X.2 support this, as these parameters both show elevated values in sites M.2 and M.3 which are known to be in proximity to a technogenic barren. Sites X.18 and X.19 also lacked a complete enough annual phenological record to undertake parameterization. Qualitative analysis of the raw data suggests similarity between these and site K.3, with all three sites only lacking spring data. Based on this evidence it seems likely that sites X.18 and X.19 are controlled by altitude. This could also provide an explanation for the outlying measured maximum NDVI at site X.17, as its proximity to site X.18 suggests it may be in an area of foothills.

Whilst the broad regional patterns of variation shown by the results of the latitudinal transect are expected, the shift from tundra parameters in the west to an increasing presence of taiga parameters in the east for the longitudinal transect is not a result which would be expected based on previous knowledge of the vegetation patterns on the Kola Peninsula. Although the vegetation maps shown in Figures 4 and 5 are not completely up-to-date, they both indicate a vegetation gradient opposite to that found here, with taiga forests showing a much more significant presence inland and to the west of the longitudinal transect, with increasing dominance of tundra towards the east of the transect in more coastal areas. These outputs for the longitudinal transect therefore cannot be explained based on current knowledge, and under the assumption that the biomization procedure is doing a good job of representing changes to surface vegetation characteristics.

Thus the results gathered from the attempted biomization of the longitudinal and latitudinal transects draw into question the extent to which the results of this study actually represent variation in the vegetation species compositions which accompany spatial biome shifts. This is difficult to assess accurately without a better basis of ground-truthing information against which to compare. However, it is possible to speculate that annual phenological profiles, and therefore parameterization variations, are controlled by a combination of the following:

i. Vegetative factors, but that these factors do not represent biome changes. This could be the case if NDVI is not sensitive enough to detect variation between areas with different species compositions. The NDVI fields used in this study are two-dimensional, and therefore have no inherent 'understanding' of the significant differences in form which exist between tundra and taiga vegetation. A key aspect of this research is that it relies on the assumption that annual variations in the multispectral characteristics of areas of tundra and taiga are significantly different due to their respective species compositions.

ii. Primarily non-vegetative factors. For example this would be the case if NDVI annual phenology responds majorly to changes in insolation related to latitude, rather than the associated vegetation growth. Based simply on the results of the latitudinal transect, an argument could be made in support of this assertion, particularly due to the very small residuals existing between the measured maximum NDVI and P6 for this transect. However the variation in the results of the longitudinal transect indicate that it is not the case that latitude is overwhelmingly the forcing factor behind parameter variation. An important consideration in this context is the fact that vegetation distributions are defined by a variety of non-vegetative factors including climate, altitude and substrate, therefore the fact that these environmental controls may influence parameterization is not unexpected. Whether or not this is problematic, or indeed at what point it becomes problematic, is less clear.

It seems apparent from the present research that the parameters resulting from annual phenologies based on NDVI are the product of various forcing factors, which are likely entangled in complex relationships. Disentangling these factors is beyond the scope of the present research – an expanded dataset would be necessary to allow a full investigation of these factors.

### 5.4 Methodological Limitations and Potential Developments

The major benefits of manually designating P1 and P2 in advance of undertaking the parameterization procedure include (i) the ability to easily identify and dismiss data sets without sufficient data around the spring greening period, and (ii) the ability to qualitatively assess more complex profiles, such as those constituent to the Monchegorsk transect, to decide whether the parameterization procedure could usefully be applied to the available data. However a reliance on manual designation of P1 and P2 limits the applicability of this methodology to greater numbers of study sites, due to the time constraints. Future work should look to develop an automated algorithm for detecting the EOW and SOS dates for phenological profiles, such that

parameterization can be rapidly undertaken for a greater number of study sites. Such automatic detection could be based on absolute changes in NDVI values relative to the total NDVI range measured at a site, or on gradients of change between two consecutive measured NDVI values, as this is readily apparent as a key feature of the spring period across almost all of the phenological profiles constructed in this study. It is likely that qualitative assessment would still need to form some part of the process due to the presence of sites exhibiting more complex patterns of NDVI change.

The calculation of P3 was modelled as a linear fit due to preliminary analysis of a limited number of annual phenological profiles such as those shown in Figures 6 and 7. However more detailed analysis across all sites following parameterization indicates that the spring greening period can follow non-linear patterns of increase. For example, at site T2.3 (Figure 28) the spring greening occurs at a slower rate initially between DOY 129 and DOY 137, before undergoing a rapid increase between DOY 137 and DOY 145. The current parameterization is unable to account for these non-linear rates of change during the spring period. Overcoming this simplification could be an area for consideration in implementing improvements to the procedure in the future.

Comparison between the measured dates of maximum NDVI and P5 values, and the measured maximum NDVI and P6 values, suggests the presence of systematic flaws in the parameterization procedure. P5 overestimates the measured date of maximum NDVI for 62 of the 73 sites for which parameterization was undertaken as a part of this study, with an average overestimation of 8.49 days for these sites. For the 11 remaining sites, the average underestimation is 2.56 days. The average overestimation across all sites is 6.82 days. These results indicate that the peak of the parameterized summer trend curves tend to fall too late in the year to reflect the measured date of peak NDVI. The most likely cause of this is considered to be asymmetry in the NDVI profile which cannot be accurately captured simply using a second-order polynomial.

Analysis of the residuals of the measured NDVI values and the calculated summer trend curve suggests the presence of an autumn trend in a significant number of the study sites. This is typified by measured NDVI values which show a brief decrease towards the end of the summer season – which is more rapid than the summer trend curve for the same time period would suggest – before stabilising to a reduced rate of decrease which is more subdued than the associated summer trend curve. This pattern can be seen to occur between DOY 241 and DOY 281 of both Figures 6 and 7, and is common to all sites within the T1, T2, F1 and F2 transects, as well as sites M.4 and M.5, and the vast majority of sites throughout the longitudinal and latitudinal transects. Designation of an end of summer date, and separate treatment of the

autumn NDVI data points following this date, offers one potential route to improving the methodology used to parameterize the phenological profile.

In contrast to P5, P6 is very likely to underestimate the measured maximum NDVI value, with this being the case for 63 of the 73 parameterized sites. The average underestimation across these 63 sites is 0.0240. Whilst maximum NDVI is only overestimated at 10 sites, the average overestimation is higher than the average underestimation, at 0.0381. The average underestimation across all sites is therefore only 0.0155. Of the 10 sites where P6 overestimates the measured maximum NDVI, 3 are sites where P5 underestimates the measured date of maximum NDVI; this does not indicate a significant relationship between the errors in these two parameters. It is considered probable that separating the data into both a summer season and an autumn season would improve the accuracy of parameterization for both P5 and P6, as the summer trend curves are currently subdued in amplitude and skewed towards later maximum dates by the presence of the autumn NDVI decrease. Designation of an end of summer date to be included in future analysis further increases the aforementioned utility of developing an automated algorithm to detect key dates in the phenological calendar. One positive factor that has become apparent in the present study is that the saturation of NDVI at high values does not appear to be an issue in studying this region of the TTE.

Although the parameterization variables constructed for this study provide enough data to address the key questions identified at the beginning of this study, they fail to capture a number of features of the NDVI profile which may usefully differentiate vegetation types. The most prominent of these is an assessment of how high NDVI is throughout the summer months, which would complement the maximum NDVI and length of summer data. Two ways to potentially improve this oversight are the calculation of a summer NDVI average, or a time-integrated greenness parameter throughout the summer period. The latter of these is recommended as being of greater utility, as the former risks undue simplification of the phenological profile which is the key unique aspect of this methodology. Recording the measured NDVI values at the start and end of summer dates could also provide useful context, both in providing a lower limit to the summer NDVI range and in considering P7, as these dates bracket the summer variation in NDVI.

As well as making changes to the parameterization aspect of the procedure, future work should also consider the thresholds for inclusion of scenes within the analysis. At present, image data is only included in further analysis if over 50% of the pixels representing a site are deemed to be of good quality. However given the paucity of data for parameterization of three of the Khibiny sites, one of the Monchegorsk sites, and three of the sites within the longitudinal

transect, it may be worth reviewing this, as decreasing the threshold may provide a greater body of results for analysis which would be more illuminating than simply missing data.

One consideration throughout any process of redeveloping the parameterization procedure should be the purpose of what is hoped to be achieved with it. Although the current parameters P5 and P6 have systematic errors in relation to the measured variables they are supposed to represent, comparison of parameterization results from sites within the tundra and taiga transects has shown them to have better discriminatory potential between the two types of biome vegetation then the associated measured variables. Promise has consequently been shown in the application of these parameters to biomization of the latitudinal transect. It is therefore suggested that whilst future research should look to make adjustments to improve the parameterization, due consideration must be given to the utility of the results for achieving research goals.

Whilst attempting to determine the vegetation of the regional transects based on parameter ranges extracted from the tundra and taiga transects shows some promise, the method remains limited in terms of the number and geographical range of input sites used to inform these ranges. The reliability of the parameter boundaries designating tundra, taiga and ambiguous areas could be improved if the control sites were to be expanded across wider areas of known vegetation cover, in order to provide a more comprehensive assessment of the biome states on the Kola Peninsula.

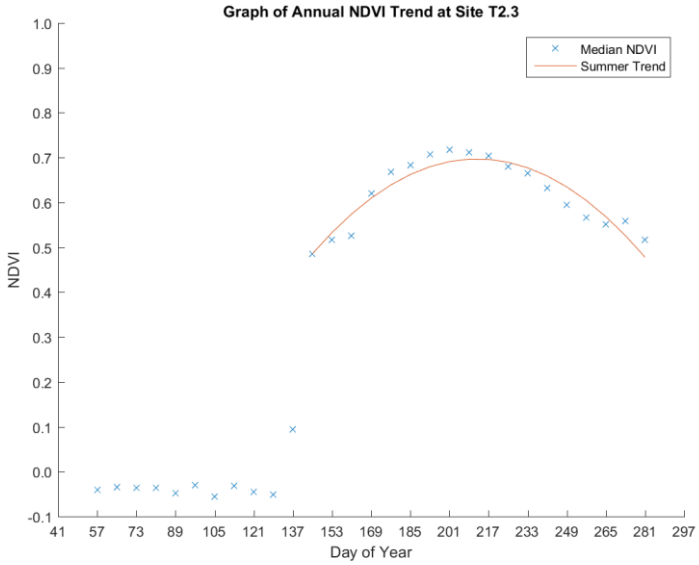


Figure 28: Graph showing the annual phenological profile for site T2.3, illustrating a non-linear rate of spring greening between DOY 129 and DOY 145.

# 6 – Further Research

Despite the methodological limitations apparent in the present study, the use of phenological profiles for differentiating between vegetation nonetheless shows impressive potential, particularly with relation to the parameter representing maximum NDVI reached. Further research should look first to optimise, and if possible standardize, the parameterization procedure for application to new research areas. Implementing the methodological improvements discussed above, and investigating the effects that these adjustments have on the results output and their utility in discriminating vegetation types, is suggested as an area for initial development. Expanding the dataset to more known areas of tundra and taiga vegetation might allow for improved quantification of the biome parameter boundaries, allowing for more reliable application to test areas through the Kola Peninsula. If possible, gathering good quality ground truthing data for comparison with the remote sensing data would facilitate improved analysis of the results of the remote sensing based method, allowing for better levels of confidence in the interpretation of future results over broader geographical areas.

The development of an automated methodology for calculating phenological parameters would allow the production of results over geographical ranges expanded beyond the discrete, linear transects used in this study. Mapping key phenological parameters as continuous data fields over a full study area is useful to visualizing variation in multiple dimensions, and can provide insight into factors affecting vegetation characteristics which are otherwise lost in point- or transect-based studies. Applying this methodology throughout the Kola Peninsula would allow enhanced identification of the spatial trends in the TTE, with the potential to enable improved understanding of the combined effects of variables including latitude, coastal proximity and altitude.

Beyond the Kola Peninsula, application of the developed parameterization procedure to different geographical areas would provide a robust test for the methodology. For example, do parameters calculated from MODIS NDVI data gathered from images of the Canadian TTE show the same potential for discriminating between tundra and taiga as has been found for the Kola Peninsula, bearing in mind the different species which are present in North America compared to European Russia? Other variables include the diverse climate, altitudinal and anthropogenic influences which are present in different Arctic regions; variations on this question should therefore be applied throughout areas of the northern hemisphere in order to test the methodology, and expand the investigation of the state and location of the TTE.

The application of a standardized methodology to other sources of remotely sensed NDVI data is considered to be a valuable and high priority research area, given the volume of recent work showing success from studying the use of complementary datasets for application

to the TTE (Montesano *et al*, 2014, 2016). Comparative assessment of the results gained from MODIS and Landsat data, with the respective benefits of greater temporal and spatial resolution, could offer future pathways to improved quantification of high latitude vegetation gradients using phenology. It has been noted that high spatial resolution data could be of particular value in areas where vegetation gradients occur over smaller horizontal extents, for example in mountainous regions. One consideration in implementing this research must be the computational intensity of analysing the much larger pixel numbers associated with Landsat data over comparable areas of MODIS data, particularly in scaling the applicability of the methodology beyond local and regional extents.

# 7 – Summary of Key Findings

- Parameterization of annual phenological profiles for selected tundra and taiga transects across the Kola Peninsula shows strong agreement between the results of constituent sites within selected biomes.
  - Taiga sites have higher winter NDVI values than tundra sites.
  - Taiga sites experience shorter springs occurring earlier in the year than tundra sites.
  - Taiga sites reach higher maximum NDVI values earlier in the year than tundra sites.
- Altitude and technogenic barrens both have significant impacts on annual phenology.
  - Both environments depress the maximum NDVI reached; this is particularly noticeable in proximity to the technogenic barren.
  - Both environments can cause data voids which inhibit the application of the parameterization procedure.
  - Qualitative assessment of the raw data for sites which could not be parameterized suggests significant differences in the missing data inhibiting parameterization.
- Attempted biomization of the longitudinal and latitudinal transect results based on parameter ranges established using the tundra and taiga transects suggests that the method has good potential, but further research is necessary to better assess the influencing factors.
  - Latitude appears to be a key control on a number of parameters, but is most closely related to the maximum NDVI reached.
  - Longitudinal variation indicates the importance of factors other than latitude in controlling parameter values, and thus the biome to which sites are related.
  - Altitude appears as a noticeable control on vegetation within both transects.
- The extent to which parameterization accurately captures variation between biomes, rather than variation related to other factors, remains uncertain.
  - Attempting to establish whether annual phenological profiles derived from NDVI accurately represents biome variation at high latitude should be a primary area of future research in order to establish the reliability of the novel methodology.
- Further research should look to fully automate the parameterization procedure, as this would facilitate rapid application of the method to new geographical ranges, in order to:
  - Improve the reliability of the parameter ranges associated with tundra and taiga.
  - Better assess the relative importance of latitude, altitude and anthropogenic influences on the outputs of the parameterization procedure.
  - Expand the research to new TTE regions, and different remote sensing datasets.

# 8 – Conclusion

The results of this study show that the parameterization of annual phenological profiles constructed using MODIS NDVI data demonstrates good potential for discriminating between different types of high latitude vegetation on the Kola Peninsula, Russia. Parameters representing the mean winter NDVI, end of winter date, start of summer date, rate of spring NDVI increase, date of maximum NDVI, and value of maximum NDVI produce identifiable ranges within each biome, based on the results of ten sites per biome split equally between two transects. The ranges of the mean winter NDVI, start of summer date, and date and value of maximum NDVI showed no overlap between the two biomes, whilst the ranges of the end of winter date and the rate of spring NDVI increase showed limited overlap. These six parameters are therefore identified as having good potential for aiding discrimination between the types of vegetation typifying each biome. The curvature of the summer trendline was the only of the seven main calculated parameters which failed to show useful discriminatory value between tundra and taiga sites.

The application of the resultant parameter boundaries to the longitudinal and latitudinal sites allowed the assignment of each parameter value to the tundra, taiga or ambiguous ranges. The output of this procedure suggested broad vegetation gradients from tundra to taiga travelling north to south along the latitudinal transect, and west to east along the longitudinal transect. The latitudinal pattern was considerably stronger than the longitudinal pattern, as would be expected based on the significant variations in environmental controls including insolation and temperature which are controlled by latitude.

A number of sites within both regional transects produced parameter outputs which were not all assigned to the same biome. It is hoped that such sites may be taken to represent regions of mixed vegetation, which would typify the tundra-taiga ecotone. However this suggestion is made tentatively – caution should be exercised as this may be indicative of a methodological failing, rather than a vegetation gradient.

The results from both of the regional transects show non-linearity in the vegetation gradients assigned based on the biomization procedure. This suggests the importance of controls on vegetation unrelated to geographical position. These controls can be at least partially attributed to variations in altitude and anthropogenic impacts, based on the limited results from the Monchegorsk and Khibiny transects. Both altitude and anthropogenic impacts have been proven to affect the annual phenological profiles of localised vegetation, perhaps most notably through depression of the maximum NDVI parameter. High altitude and technogenic barrens both produce gaps in the availability of good quality MODIS NDVI data which inhibit the application of parameterization.

This methodology is considered to have good potential for discriminating vegetation types due to its ability to capture geographical variation in key phenological parameters. However the extent to which these variations can be taken to represent variation between biomes is unclear. The effects of other factors, both vegetative and non-vegetative, should not be dismissed. However these factors cannot be adequately assessed using the relatively limited results of this study, therefore additional research will be necessary to further explore the discriminatory potential identified in this research.

It is suggested that future research in this area initially focusses on refining the parametrization procedure. It is considered likely that identifying autumn trends separately to summer trends will improve the agreement between parameterized and measured dates and values of maximum NDVI. Full automation should be the aim; this will involve constructing a quantitative means of calculating key seasonal dates related to the end of winter, start of summer and end of summer. Following improvements to the procedure, parameterization should be applied to an expanded range of sites, in order to improve understanding of the parameter ranges produced by areas of known tundra and taiga vegetation.

The eventual goal is to develop a robust methodology which can be applied to broad areas of the northern hemisphere in order to automatically assess biome ranges, and therefore the likely location and extent of the tundra-taiga ecotone. This goal is currently very distant, and a number of methodological improvements will be required before the extent of its feasibility can be known. The value of the work undertaken in this study is in its illustration of the significant potential of the methodology, which shows its viability and indicates the importance of further research into its application.

# Bibliography

Apps, M.J., Kurz, W.A., Luxmoore, R.J., Nilsson, L.O., Sedjo, R.A., Schmidt, R., Simpson, L.G. and Vinson, T.S. (1993) Boreal forests and tundra. *Water, Air and Soil Pollution*; **70**(1-4); 39-53.

Beck, P.S.A., Juday, G.P., Alix, C., Barber, V.A., Winslow, S.E., Sousa, E.E., Heiser, P., Herriges, J.D. and Goetz, S.J. (2011) Changes in forest productivity across Alaska consistent with biome shift. *Ecology Letters*; **14**(4); 373-379.

Beck, P.S.A., Jonsson, P., Hogda, K.-A., Karlsen, S.R., Eklundh, L. and Skidmore, A.K. (2007) A ground-validated NDVI dataset for monitoring vegetation dynamics and mapping phenology in Fennoscandia and the Kola peninsula. *International Journal of Remote Sensing*; **28**(19); 4311-4330.

Beringer, J., Chapin III, F.S., Thompson, C.C. and McGuire, A.D. (2005) Surface energy exchanges along a tundra-forest transition and feedbacks to climate. *Agricultural and Forest Meteorology*; **131**; 143-161.

Billings, W.D. (1987) Carbon balance of Alaskan tundra and taiga ecosystems: past, present and future. *Quaternary Science Reviews*; **6**(2); 165-177.

Blinova, T. and Chmielewski, F.M. (2015) Climatic warming above the Arctic Circle: are there trends in timing and length of the thermal growing season in Murmansk Region (Russia) between 1951 and 2012? *International Journal of Biometeorology*; **59**(6); 693-705.

Bonan, G.B., Chapin III, F.S. and Thompson, S.L. (1995) Boreal forest and tundra ecosystems as components of the climate system. *Climatic Change*; **29**(2); 145-167.

Bonan, G.B., Pollard, D. and Thompson, S.L. (1992) Effects of boreal forest vegetation on global climate. *Nature*; **359**; 716-717.

Bradshaw, C.J.A. and Warkentin, I.G. (2015) Global estimates of boreal forest carbon stocks and flux. *Global and Planetary Change*; **128**; 24-30.

Callaghan, T.V., Crawford, R.M.M., Eronen, M., Hofgaard, A., Payette, S., Rees, W.G., Skre, O., Sveinbjornsson, B., Vlassova, T.K. and Werkman, B.R. (2002) The dynamics of the tundra-taiga boundary: an overview and suggested coordinated and integrated approach to research. *Ambio*; Special Report Number 12; pp.3-5.

Chernen'kova, T.V., Puzachenko, M.Y., Koroleva, N.E. and Basova, E.V. (2013) Assessment of forest spatial differentiation in Murmansk Province using field surveys and remote sensing data. *Contemporary Problems of Ecology*; **6**(7); 746-754.

Crawford, R.M.M., Jeffree, C.E. and Rees, W.G. (2003) Paludification and forest retreat in northern oceanic environments. *Annals of Botany*; **91**(2); 213-226.

Daffern, C.J. (2017) *Using satellite remote sensing to investigate phenological variability between tundra and taiga landscapes.* MPhil (Short Essay). University of Cambridge.

Daffern, C.J. (2016) *Discuss how satellite remote sensing data can be used to identify the location and form of the tundra-taiga ecotone*. MPhil (Short Essay). University of Cambridge.

Deluca, T.H. and Boisvenue, C. (2012) Boreal forest soil carbon: distribution, function and modelling. *Forestry*; **85**(2); 161-184.

Demin, V.I. and Zyuzin, Y.L. (2006) On climatic changes in the Khibiny Mountains (Kola Peninsula, Russia). *Physics of Auroral Phenomena*, Proc. XXIX Annual Seminar, Apatity; 281-284. [online] Accessed on: 31.05.2017. Available at: http://pgia.ru:81/seminar/archive/2006/6_atm/demin.pdf.

EU Interact (2017) *Khibiny Educational and Scientific Station*. [online] Accessed on: 31.05.2017. Available at: http://www.eu-interact.org/field-sites/russia/khibiny/

Gervais, B.R., MacDonald, G.M., Snyder, J.A. and Kremenetski, C.V. (2002) *Pinus Sylvestris* treeline development and movement on the Kola Peninsula of Russia: pollen and stomate evidence. *Journal of Ecology*; **90**; 627-638.

Gervais, B.R. and MacDonald, G.M. (2001) Modern pollen and stomate deposition in lake surface sediments from across the treeline on the Kola Peninsula, Russia. *Review of Palaeobotany and Palynology*; **114**(3-4); 223-237.

Hadi, Korhonen, L., Hovi, A., Ronnholm, P. and Rautiainen, M. (2016) The accuracy of large-area forest canopy cover estimation using Landsat in boreal region. *International Journal of Applied Earth Observation and Geoinformation*; **53**; 118-127.

Harden, J.W., O'Neill, K.P., Trumbore, S.E., Veldhuis, H. and Stocks, B.J. (1997) Moss and soil contributions to the annual net carbon flux of a maturing boreal forest. *Journal of Geophysical Research, Atmospheres*; **102**(D24); 28805-28816.

Harding, R., Kuhry, P., Christensen, T.R., Sykes, M.T., Dankers, R. and van der Linden, S. (2002) Climate feedbacks at the tundra-taiga interface. *Ambio*; Special Report Number 12; pp.47-55.

Heiskanen, J. (2006) Tree cover and height estimation in the Fennoscandian tundra-taiga transition zone using multiangular MISR data. *Remote Sensing of Environment*; **103**(1); 97-114.

Hofgaard, A., Tommervik, H., Rees, G. and Hanssen, F. (2013) Latitudinal forest advance in northernmost Norway since the early 20$^{th}$ century. *Journal of Biogeography*; **40**(5); 938-949.

Hopkinson, C., Chasmer, L., Barr, A.G., Kljun, N., Black, T.A. and McCaughey, J.H. (2016) Monitoring boreal forest biomass and carbon storage change by integrating airborne laser scanning, biometry and eddy covariance data. *Remote Sensing of Environment*; **181**; 82-95.

Houghton, R.A., Butman, D., Bunn, A.G., Krankina, O.N., Schlesinger, P. and Stone, T.A. (2007) Mapping Russian forest biomass with data from satellites and forest inventories. *Environmental Research Letters*; **2**(4); 045032.

Jobbagy, E.G. and Jackson, R.B. (2000) The vertical distribution of soil organic carbon and its relation to climate and vegetation. *Ecological Applications*; **10**(2); 423-436.

Kauppi, P.E., Rautiainen, A., Korhonen, K.T., Lehtonen, A., Liski, J., Nojd, P., Tuominen, S., Haakana, M. and Virtanen, T. (2010) Changing stock of biomass carbon in a boreal forest over 93 years. *Forest Ecology and Management*; **259**(7); 1239-1244.

Kharuk, V., Ranson, K. and Dvinskaya, M (2007) Evidence of evergreen conifer invasion into larch dominated forests during recent decades in central Siberia. *Eurasian Journal of Forest Research*; **10**(2); 163-171.

Koroleva, N.E. (1994) Phytosociological survey of the tundra vegetation of the Kola Peninsula, Russia. *Journal of Vegetation Science*; **5**(6); 803-812.

Kozlov, M.V. and Berlina, N.G. (2002) Decline in length of the summer season on the Kola Peninsula, Russia. *Climatic Change*; **54**(4); 387-398.

Kravtsova, V.I. and Loshkareva, A.R. (2013) Dynamics of vegetation in the tundra-taiga ecotone on the Kola Peninsula depending on climate fluctuations. *Russian Journal of Ecology*; **44**(4); 303-311.

Kremenetski, C., Vaschalova, T. and Sulerzhitsky, L. (1999) The Holocene vegetation history of the Khibiny Mountains: implications for the post-glacial expansion of spruce and alder on the Kola Peninsula, north-western Russia. *Journal of Quaternary Science*; **14**(1); 29-43.

Loranty, M.M., Goetz, S.J. and Beck, P.S.A. (2011) Tundra vegetation effects on pan-Arctic albedo. *Environmental Research Letters*; **6**(2); 029601.

Lundberg, A. and Beringer, J. (2005) Albedo and snowmelt rates across a tundra-to-forest transition. *15th International Northern Research Basins Symposium and Workshop.* Lulea to Kvikkjokk, Sweden. 29th August – 2nd September 2005. Available at: https://www.diva-portal.org/smash/get/diva2:1008800/FULLTEXT01.pdf. Accessed on: 15.05.2017.

MacDonald, G.M., Kremenetski, K.V. and Beilman, D.W. (2008) Climate change and the northern Russian treeline zone. *Philosophical Transactions of the Royal Society B: Biological Sciences*; **363**(1501); 2285-2299.

Mack, M.C., Schuur, E.A.G., Bret-Harte, M.S., Shaver, G.R. and Chapin III, F.S. (2004) Ecosystem carbon storage in arctic tundra reduced by long-term nutrient fertilization. *Nature*; **431**; 440-443.

Malhi, Y., Baldocchi, D.D. and Jarvis, P.G. (1999) The carbon balance of tropical, temperate and boreal forests. *Plant, Cell & Environment*; **22**; 715-740.

Marshall, G.J., Vignols, R.M., and Rees, W.G. (2016) Climate change in the Kola Peninsula, Arctic Russia, during the last 50 years from meteorological observations. *Journal of Climate*; **29**(18); 6823-6840.

MathWorks (2015) MATLAB (Version R2015b) [computer program] The MathWorks, Inc., Natick, Massachusetts. Accessed on: 21.11.2016. Available at: https://www.mathworks.com/products/matlab.html.

Montesano, P.M., Neigh, C.S.R., Sexton, J., Feng, M., Channan, S., Ranson, K.J. and Townshend, J.R. (2016) Calibration and validation of Landsat tree cover in the taiga-tundra ecotone. *Remote Sensing*; **8**(7); 551-567.

Montesano, P.M., Nelson, R.F., Dubayah, R.O., Sun, G., Cook, B.D., Ranson, K.J.R., Næsset, E. and Kharuk, V. (2014) The uncertainty of biomass estimates from LiDAR and SAR across a boreal forest structure gradient. *Remote Sensing of Environment*; **154**; 398-407.

Montesano, P.M., Nelson, R., Sun, G., Margolis, H., Kerber, A. and Ranson, K.J. (2009) MODIS tree cover validation for the circumpolar tundra-taiga transition zone. *Remote Sensing of Environment*; **113**(10); 2130-2141

NASA LP DAAC (2016) Vegetation Indices 16-Day L3 Global 250m MOD13Q1 and MYD13Q1, Version 005. [online] NASA EOSDIS Land Processes DAAC, USGS Earth Resources Observation and Science (EROS) Center, Sioux Falls, South Dakota (https://lpdaac.usgs.gov). Accessed on: 14.02.2017. Available at: https://lpdaac.usgs.gov/dataset_discovery/modis/modis_products_table.

NASA LP DAAC (2014) Land Water Mask Derived from MODIS and SRTM L3 Global 250m SIN Grid, Version 005. [online] NASA EOSDIS Land Processes DAAC, USGS Earth Resources Observation and Science (EROS) Center, Sioux Falls, South Dakota (https://lpdaac.usgs.gov). Accessed on: 17.02.2017. Available at: https://lpdaac.usgs.gov/dataset_discovery/modis/modis_products_table/mod44w.

NASA LP DAAC (2011) MODIS Reprojection Tool (Version 4.1) [computer program] USGS Earth Resources Observation and Science (EROS) Center, Sioux Falls, South Dakota. Accessed on: 13.02.2017. Available at: https://lpdaac.usgs.gov/tools/modis_reprojection_tool.

Orlova, M.A., Lukina, N.V., Tutubalina, O.V., Smirnov, V.E., Isaeva, L.G. and Hofgaard, A. (2013) Soil nutrient's spatial variability in forest-tundra ecotones on the Kola Peninsula, Russia. *Biogeochemistry*; **113**(1); 283-305.

Pan, Y., Birdsey, R.A., Fang, J., Houghton, R., Kauppi, P.E., Kurz, W.A., Phillips, O.L., Shvidenko, A., Lewis, S.L., Canadell, J.G., Ciais, P., Jackson, R.B., Pacala, S.W., McGuire, A.D., Piao, S., Rautiainen, A., Sitch, S., and Hayes, D. (2011) A large and persistent carbon sink in the world's forests. *Science*; **333**(6045); 988-993.

Park, T., Ganguly, S., Tommervik, H., Euskirchen, E.S., Hogda, K.-A., Karlsen, S.R., Brovkin, V., Nemani, R.R. and Myneni, R.B. (2016) Changes in growing season duration and productivity of northern vegetation inferred from long-term remote sensing data. *Environmental Research Letters*; **11**(8); 084001.

Post, W.M., Emanuel, W.R., Zinke, P.J. and Stangenberger, A.G. (1982) Soil carbon pools and world life zones. *Nature*; **298**; 156-159.

Ranson, K.J., Montesano, P.M. and Nelson, R. (2011) Object-based mapping of the circumpolar taiga-tundra ecotone with MODIS tree cover. *Remote Sensing of Environment*; **115**(12); 3670-3680.

Ranson, K.J., Sun, G., Kharuk, V.I. and Kovacs, K. (2004) Assessing tundra-taiga boundary with multi-sensor satellite data. *Remote Sensing of Environment*; **93**(3); 283-295.

Rees, W.G. and Williams, M. (1997) Monitoring changes in land cover induces by atmospheric pollution in the Kola Peninsula, Russia, using Landsat-MSS data. *International Journal of Remote Sensing*; **18**(8); 1703-1723.

Saich, P. Rees, W.G. and Borgeaud, M. (2001) Detecting pollution damage to forests in the Kola Peninsula using the ERS SAR. *Remote Sensing of the Environment*; **75**(1); 22-28.

Sexton, J.O., Song, X.-P., Feng, M., Noojipady, P., Anand, A., Huang, C., Kim, D.-O., Collins, K.M., Channan, S., DiMiceli, C. and Townshend, J.R. (2013) Global, 30-m resolution continuous fields of tree cover: Landsat-based rescaling of MODIS vegetation continuous fields with lidar-based estimates of error. *International Journal of Digital Earth*; **6**(5); 427-448.

Shipigina, E. and Rees, W.G. (2012) Analysis of human impact on boreal vegetation around Monchegorsk, Kola Peninsula, using automated remote sensing technique. *Polar Record*; **48**(244); 94-106.

Schwartz, M. D. and Reed, B. C. (1999) Surface phenology and satellite sensor-derived onset of greenness: an initial comparison. *International Journal of Remote Sensing*; **20**; 3451–3457.

Sparks, T.H. and Menzel, A. (2002) Observed changes in seasons: an overview. *International Journal of Climatology*; **22**(14); 1715-1725.

Sturm, M., Douglas, T., Racine, C. and Liston, G.E. (2005) Changing snow and shrub conditions affect albedo with global implications. *Journal of Geophysical Research, Biogeosciences*; **110**(G1); G01004.

Sveinbjornsson, B., Hofgaard, A. and Lloyd, A. (2002) Natural causes of the tundra-taiga boundary. *Ambio*; Special Report Number 12; pp.23-29.

Tarnocai, C., Canadell, J.G., Schuur, E.A.G., Kuhry, P., Mazhitova, G. and Zimov, S. (2009) Soil organic carbon pools in the northern circumpolar permafrost region. *Global Biogeochemical Cycles*; **23**(2); GB2023.

USGS (2015) *Deriving phenological metrics from NDVI*. [online] Available at: https://phenology.cr.usgs.gov/methods_metrics.php. Accessed on: 18.05.2017.

USGS (2010) Global Multi-resolution Terrain Elevation Data 2010 (GMTED2010). [online] Accessed on: 15.02.2017. Available at: https://lta.cr.usgs.gov/GMTED2010.

Virtanen, R., Oksanen, L., Oksanen, T., Cohen, J., Forbes, B.C., Johansen, B., Kayhko, J., Olofsson, J., Pulliainen, J. and Tommervik, H. (2016) Where do the treeless tundra areas of northern highlands fit in the global biome system: toward an ecologically natural subdivision of the tundra biome. *Ecology and Evolution*; **6**(1); 143-158.

Vlassova, T.K. (2002) Human impacts on the tundra-taiga zone dynamics: the case of the Russian lesotundra. *Ambio*; Special Report Number 12; pp.30-36.

Wang, Y.P. and Polglase, P.J. (1995) Carbon balance in the tundra, boreal forest and humid tropical forest during climate change: scaling up from leaf physiology and soil carbon dynamics. *Plant, Cell and Environment*; **18**(10); 1226-1244.